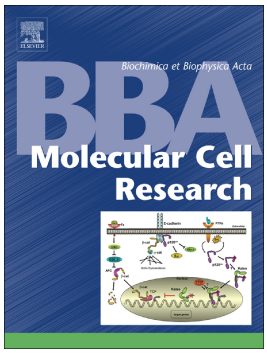

Ceramide induces a multicomponent intracellular calcium increase triggering the acrosome secretion in human sperm

Cintia Celina Vaquer, Laila Suhaiman, Martín Alejandro Pavarotti, Gerardo Andrés De Blas, Silvia Alejandra Belmonte

PII: S0167-4889(20)30062-8

DOI: https://doi.org/10.1016/j.bbamcr.2020.118704

Reference: BBAMCR 118704

To appear in: *BBA - Molecular Cell Research*

Received date: 1 December 2019

Revised date: 11 March 2020

Accepted date: 12 March 2020

Please cite this article as: C.C. Vaquer, L. Suhaiman, M.A. Pavarotti, et al., Ceramide induces a multicomponent intracellular calcium increase triggering the acrosome secretion in human sperm, *BBA - Molecular Cell Research* (2020), https://doi.org/10.1016/j.bbamcr.2020.118704

Ceramide induces a multicomponent intracellular calcium increase triggering the acrosome secretion in human sperm

Cintia Celina Vaquer[a1], Laila Suhaiman[b1], Martín Alejandro Pavarotti[a], Gerardo Andrés De Blas[a,c], Silvia Alejandra Belmonte[a,c,*]

[a]Instituto de Histología y Embriología de Mendoza (IHEM) "Dr. Mario H. Burgos". CONICET. Universidad Nacional de Cuyo. 5500 Mendoza, Argentina.

[b]Instituto Interdisciplinario de Ciencias Básicas (ICB) CONICET. Universidad Nacional de Cuyo. 5500 Mendoza, Argentina.

[c]Facultad de Ciencias Médicas, Universidad Nacional de Cuyo, Mendoza, Argentina

[1] Both authors contributed equally to this work.

***Corresponding Author:** Silvia A. Belmonte Instituto de Histología y Embriología (IHEM) CONICET, Facultad de Ciencias Médicas, Universidad Nacional de Cuyo, 5500, Mendoza, Argentina.

Telephone: +54-261-449-4143, ext 7015

E-mail:belmonte.silviaalejandra@gmail.com,

sbelmonte@mendoza-conicet.gob.ar

Authors' emails

Cintia Celina Vaquer: vaquer.cintia@gmail.com

Laila Suhaiman: laila.suhaiman@gmail.com

Martin Alejandro Pavarotti: martinpavarotti@gmail.com

Gerardo Andrés De Blas: gerardo.deblas@gmail.com

Abstract

Exocytosis of spermatozoon's secretory vesicle, named acrosome reaction (AR), is a regulated event that plays a central role in fertilization. It is coupled to a complex calcium signaling. Ceramide is a multitasking lipid involved in exocytosis. Nevertheless, its effect on secretion is controversial and the underlying cellular and molecular mechanisms remain unknown. Human spermatozoa are useful to dissect the role of ceramide in secretion given that the gamete is not capable to undergo any trafficking mechanisms other than exocytosis. We report for the first time, the presence of sphingolipid metabolism enzymes such as neutral-sphingomyelinase and ceramide synthase in sperm. Ceramidases are also present and active. Both the addition of cell-permeable ceramide and the rise of the endogenous one, increase intracellular calcium acting as potent inducers of exocytosis. Ceramide triggers AR in capacitated spermatozoa and enhances the gamete response to progesterone. The lipid induces physiological ultrastructural changes in the acrosome and triggers an exocytosis-signaling cascade involving protein tyrosine

phosphatase 1B and VAMP2. Real-time imaging showed an increment of calcium in the cytosol upon ceramide treatment either in the absence or in the presence of extracellular calcium. Pharmacological experiments demonstrate that at early stages the process involves ryanodine receptors, CatSper (calcium channel of sperm), and store-operated calcium channels.

We set out the signaling sequence of events that connect ceramide to internal calcium mobilization and external calcium signals during secretion. These results allow the coordination of lipids and proteins in a pathway that accomplishes secretion. Our findings contribute to the understanding of ceramide's role in regulated exocytosis and fertilization.

Keywords. Acrosome reaction, Calcium, Ceramide, Exocytosis, Lipid signaling, Sperm

Abbreviations

AR, acrosome reaction; C6-Cer, ceramide; S1P, sphingosine 1-phosphate; SM, sphingomyelin; nSMase, neutral sphingomyelinase, CDase, ceramidase; SK, sphingosine kinase; FITC-PSA, FITC-coupled Pisum sativum agglutinin; Fluo3-AM, 1-[2-Amino-5-(2,7-dichloro-6-hydroxy-3-oxo-9-xanthenyl)phenoxy]-2-(2-amino-5-methylphenoxy) ethane-N,N,N',N'-tetraacetic acid, pentaacetoxymethyl ester; IP_3, inositol 1, 4, 5 triphosphate; EGTA-AM, EGTA acetoxymethyl ester;

TEM, transmission electron microscopy; PTP1B, protein tyrosine phosphatase 1B; SLO, streptolysin O; YM, 4-methyl-4'-[3,5-bis(trifluoromethyl)-1H-pyrazol-1-yl]-1,2,3-thiadiazole-5-carboxanilide; SKF, 1-[b-[3-(4-methoxyphenyl)propoxy]-4-methoxyphenethyl]-1H-imidazole; XC, xestospongin C; 2-APB, 2-aminoethoxy-diphenylborate; PMA, phorbol 12-myristate 13-acetate; DAG, diacylglycerol; RR, rutenium red; C12-NBD, N-lauroyl-D-erythro-sphingosine Nitro-2-1,3-BenzoxaDiazole-4-yl, D-NMAPPD (1R,2R)-2-N-myristoylamino-1-(4-nitrophenyl)-1,3-propandiol.

1. Introduction

A human spermatozoon is a terminal specialized cell that has the only function of fertilizing an oocyte to pass on the genetic information contained in its nucleus. When it reaches the egg, progesterone stimulates the release of the acrosome's granule content. Exocytosis of the acrosome, named acrosome reaction (AR), is a calcium-regulated secretion required to fertilize the egg. Each sperm possess a single, large, and electron-dense vesicle that, in response to exocytosis inducers, swells to contact the plasma membrane, attaches to and fuses with it. Finally, it detaches entirely, together with the part of the plasma membrane that surrounds it. A complex calcium signaling governs these events. First, a transitory calcium influx through plasma

membrane channels leads to intracellular calcium mobilization. The emptying of intracellular reservoirs provokes the opening of store-activated calcium channels present at the plasma membrane triggering a sustained calcium increase [1,2,3].

Sphingolipids constitute ~10–20% of total membrane lipids [4]. Ceramide is the central hub of sphingolipid metabolism given that it can be synthesized *de novo* from the condensation of palmitate and serine or generated via the hydrolysis of sphingomyelin (SM) as a result of sphingomyelinase (SMase) activation, the last, known as the SM pathway. Ceramide can be used to synthesize other interconnected bioactive lipids thus orchestrating cellular responses (for a review see [5]). The sphingolipid metabolites ceramide, sphingosine 1-phosphate (S1P), and ceramide 1-phosphate (C1P) are essential signaling molecules involved in the regulation of multiple physiological functions including exocytosis (Reviewed in [6]).

Ceramides are multitasking sphingolipids whose effects can be analyzed from different standpoints. It affects the biophysical properties of membranes (For a review see [7]) and are important participants of signal transduction. Numerous intracellular targets have been found for ceramide, particularly kinases and phosphatases [8]. The effect of ceramide on the cytoplasmic calcium concentration differs according to the cell type and many studies report the relationship between ceramide and calcium

channels e.g., in rat pinealocytes, the lipid inhibits L-type calcium channel [9]. Besides, the addition of ceramide increases cytoplasmic [Ca^{2+}] due to the release of calcium from intracellular reservoirs [10,11,12,13].

The sphingolipid effect on exocytosis is controversial. On one hand, an inhibitory effect of cell-permeable ceramides on exocytosis has been observed in granulocytes and a cell-free system [14,15]. In rat PC12 cells, the differential effect of ceramides on exocytosis depends on the length of the fatty acid chain [16]. Ji et al. (2011) demonstrated that ceramide elicits serotonin release from mast cells [17]. Even though ceramide affects the exocytosis, the molecular mechanism underlying has not been elucidated yet.

Spermatozoa is a terminal cell lacking almost all organelles, transcriptional, and translational activity. They are fated for a single membrane fusion event, the exocytosis of the acrosome. This feature is especially helpful to analyze in detail the function of a multitasking lipid as ceramide in secretion.

Sperm treatment with sphingomyelinase and the consequent generation of ceramides, or addition of exogenous ceramides increases the percentage of progesterone-sensitive and spontaneously reacted sperm [18]. Murase et al, (2004) described that in boar spermatozoa, calcium ionophore-induced acrosome secretion was enhanced by ceramide [19].

A few years ago, we demonstrated that S1P triggers AR in human sperm activating a Gi-coupled receptor through an autocrine/paracrine action [20]. Taking into account these findings, we hypothesize that ceramide, the almost immediate precursor of S1P, could be somehow regulating the exocytosis of the acrosome by using this pathway or exerting an effect by its own.

Here, we present the first report showing the presence, localization, and activity of some enzymes of the sphingolipid metabolism in human spermatozoa. This study aims to establish whether ceramide is affecting the sperm exocytosis and if so, to reveal the molecular mechanism/s regulated by this lipid. We report that both addition of cell-permeable ceramide and the rise of the endogenous one, increase intracellular calcium concentration, and act as potent inducers of the acrosome content release in human spermatozoa. Here we present profuse evidence demonstrating how ceramide coordinates a signaling network to achieve the AR. Our findings suggest that this exocytic process may be shared with that induced by physiological and pharmacological stimuli raising the importance of ceramide concentration in human sperm membranes during fertilization.

2. Materials and methods

2.1. Reagents

Human Tubal Fluid medium [HTF] contains 5.94 g/L NaCl, 0.35 g/L KCl, 0.05 g/L $MgSO_4$.$7H_2O$, 0.05 g/L KH_2PO_4, 0.3 g/L $CaCl_2$.$2H_2O$, 2.1 g/L $NaHCO_3$, 0.51 g/L D-glucose, 0.036 g/L Na pyruvate, 2.39 g/L Na lactate, 0.06 g/L penicillin, 0.05 g/L streptomycin, 0.01 g/L phenol red. 2-aminoethoxydiphenylborate (2-APB) and sphingosine kinase inhibitor (SKI) were from Calbiochem (MERCK Química Argentina SAIC, Buenos Aires, Argentina). C6-ceramide was from Avanti Polar Lipids, Inc. (Alabaster, AL, USA). TLC aluminum sheets silica gel 60 were from MERCK KGaA (Darmstadt, Germany). Verapamil, 4-methyl-4'-[3,5-bis(trifluoromethyl)-1H-pyrazol-1-yl]-1,2,3-thiadiazole-5-carboxanilide (YM-58483) and 1-[b-[3-(4-methoxyphenyl)propoxy]-4-methoxyphenethyl]-1H-imidazole (SKF-96365), xestospongin C, phorbol 12-myristate 13-acetate (PMA), and progesterone were from Sigma (Sigma-Aldrich Argentina SA, Buenos Aires, Argentina). A23187 was from Alomone (Alomone Labs. Ltd. Jerusalem, Israel). Albumin and fluorescein-isothiocyanate-coupled Pisum sativum lectin were from ICN (Eurolab SA, Buenos Aires, Argentina). Horseradish Peroxidase [HRP] coupled anti-rabbit antibody and Cy3 labeled goat anti-rabbit antibody were from Jackson Immunochemicals (Sero-immuno Diagnostics, Inc. Tucker, GA, USA). Rutenium red, N-lauroyl-D-erythro-sphingosine Nitro-2-1,3-BenzoxaDiazole-4-yl (C12-NBD), (1R,2R)-2-N-myristoylamino-

1-(4-nitrophenyl)-1,3-propandiol (D-NMAPPD), ionomicyn, 1,2-bis (o-aminophenoxy)ethane-N,N,N0,N0-tetraacetic acid (BAPTA), and glycine, 4-(6-Acetoxymethoxy-2,7-dichloro-3-oxo-9-xanthenyl)-4′-methyl-2,2′(ethylenedioxy)dianiline-N,N,N′,N′-tetraacetic acid tetrakis(acetoxymethyl) ester (Fluo-3 AM) were from Molecular Probes (Invitrogen Argentina). All electron microscopy supplies were from Ted Pella Inc. Recombinant SLO was obtained from Dr. Bhakdi (University of Mainz, Mainz, Germany). All other chemicals were purchasedfrom Genbiotech or Tecnolab.

2.2. Ethics Approval

Data collection followed the principles outlined in the Declaration of Helsinki; all donors signed an informed consent agreeing to supply their own anonymous information and semen samples. The Ethics Committee of the Medical School, Universidad Nacional de Cuyo, approved the signed informed consent and the protocol for semen handling.

2.3. Sperm acrosome exocytosis assays

Healthy donors provided human semen samples (age range: 25- to 35-years old). We only included in the analysis, samples that met the quality parameters accepted by the World Health Organization [WHO]. At least 2 days of sexual abstinence are required to obtain the samples. We incubated the semen for 30 min at 37°C to allow its liquefaction. We recovered highly motile spermatozoa

after a swim-up separation for 1 h in HTF medium supplemented with 5 mg/ml of bovine serum albumin when indicated (capacitating medium) at 37°C in an atmosphere of 5% CO_2/95% air. For non-capacitated sperm, we used HTF without BSA for both the swim-up and after swim-up incubations. We adjusted cell concentration to 5-10 × 10^6 sperm/ml with HTF, and then we incubated them under capacitating conditions for at least 2 hours. After that treatment, we processed the samples for Western blot, AR assays, calcium measurements, and enzyme activities. We evaluated the acrosomal status by FITC-PSA staining according to [21] and as described in detail in our previous publications [20,22,23]. We scored at least 300 cells using a Nikon microscope equipped with epifluorescence optics. In all experiments, we included negative (no stimulation) and positive controls (stimulated with A23187, progesterone, DAG, or PMA).

In humans, the PTPN1 gene encodes the tyrosine-protein phosphatase non-receptor type 1 also known as protein-tyrosine phosphatase 1B (PTP1B). In some cases, we preincubated spermatozoa for 10 min at 37°C with photoinhibitable reagents for this enzyme, as photosensitive-PTP inhibitor I (PTPi), before adding a stimulus like progesterone or C6-Cer. All these procedures were carried out in the dark. We induced photolysis by exposing twice (1 min each time) to a UV transilluminator

[24,25]. The acrosome reaction was evaluated as described before.

2.4. SDS-PAGE and Western blot

Sperm were processed as described in the following publications [20,24,26]. Then we incubated the blots with anti-nSMase, anti-nCDase, anti-CerS, or anti-ACER (2 μg/ml, rabbit polyclonal Aviva Systems Biology), for 2 h at RT. We used horseradish peroxidase-conjugated anti-rabbit as a secondary antibody (0.1 μg/ml). We removed excess first and second antibodies by washing 5 × 5 min in PBS, pH 7.6, 0.1% Tween 20. We performed detection with a chemiluminescence system: Kallium Technologies, Buenos Aires, Argentina) by using a Luminescent Image Analyzer LAS-4000.

2.5. Indirect Immunofluorescence and Confocal microscopy

We spotted capacitated sperm on slides covered with poly-L-lysine. Then we fixed the cells in 2% paraformaldehyde at RT. Then, we followed the protocol set up in our laboratory described in Suhaiman et al. (2010) [20]. We incubated sperm with specific antibodies: anti-nSMase2 (20 μg/ml); anti-nCDase (20 μg/ml), anti-aCER (20 μg/ml), or anti-CerS (20 μg/ml) overnight at 4°C. As a secondary antibody we used Cy3-labeled anti-rabbit (1:600 in 1% bovine serum-PBS). Finally, we fixed the cells in cold methanol for 1 min and stained with FITC-PSA. We observed the cells by confocal microscopy (Olympus FluoViewTM FV1000

confocal microscope, Olympus, Argentina), with the FV10-ASW software. We processed the images with MetaMorph, Image J and Corel Draw.

2.6. Transmission Electron Microscopy

We incubated capacitated sperm with 10 μM C6-ceramide or 10 μM A23187, as a positive control, at 37°C for 15 min. A sample without any treatment was included as a negative control. We washed sperm twice in warm PBS and fixed in 2.5% v/v glutaraldehyde in 0.1 M sodium cacodylate buffer for 2 h at 10 °C. We obtained the sperm pellet by centrifugation for 30 sec at 10,000 rpm. We further fixed the pellets in 1% OsO4 for 1h at RT. We dehydrated samples in a graded acetone series and embedded in low-viscosity epoxy resin. We performed resin polymerization at 70°C for 48 h. We obtained ultrathin sections with an interference color gray by using a diamond knife in an ultramicrotome (Ultracut R; Leica, Austria). We collected ultrathin sections on 200-mesh copper grids and stained with uranyl acetate and lead citrate as described in [27,28]. We observed the samples under the electron microscope (model 900; Zeiss, Jena, Germany) at 80 kV. Micrographs were obtained with a Gatan Orius SC1000 (model 832) charge-coupled device. A. Morales, Ph.D. and P. López, MS from the STAN: ST3371 of TEM and SEM samples preparation, IHEM-CONICET-UNCuyo processed the samples. We scored at least 100 cells per condition

and classified acrosomal patterns as intact, swollen (swollen and waving), reacted (lost and vesiculated acrosomes). We analyzed the data by using the Newman-Keuls Multiple Comparison Test and the program GraphPad Prism 5. We considered significant differences at the $p<0.05$ level.

2.7. Cell-penetrating peptides conjugation with Tetanus toxin

The protein was obtained as described in Mayorga et al, (2019) [29]. Briefly, we transformed into E. coli XL-1Blue (Stratagene) the plasmid's DNA encoding 6His-tetanus toxin light chain (pQE3plasmid, Qiagen). We induced protein expression overnight at 20°C with 0.2 mM isopropyl 1-thio-D-galactopyranoside. We purified the 6His-tagged proteins according to the QIAexpressionist (www.qiagen.com). Conjugation between tetanus toxin and the CPP peptides (KRRRRRRRRRC) was performed using Trilinks Biotechnology Kits, according to the manufacturer's instruction. The procedure is described in detail in Mayorga et al. (2019) [29]. We confirmed purity by SDS-PAGE analysis.

2.8. Ceramidase activity measurement

We determined ceramidase activity as described in Tada et al (2010) [30] and modified the method for sperm. Briefly, cells (100×10^6) were incubated with 10 μM C12-NBD delivered in 4 mg/ml fatty acid-free BSA (FAF-BSA) for 1 h at 37°C. Sperm were kept in the dark to avoid NBD degradation. Then, we

washed sperm in HTF/0.4% FAF-BSA. We added phosphatase inhibitors: 15 mM NaF and 1 mM sodium orthovanadate. When indicated, we treated sperm with 10 μM D-NMPPAD (ceramidase inhibitor) for 20 min at 37°C. After that, we added A23187 and incubated for 20 min. We stopped the reaction with 250 μl chloroform, 500 μl methanol, and mixed. Subsequently, we added 500 μl chloroform and 250 μl of water. We centrifuged the sperm at 600 × g for 10 min. C12-NBD is found in the organic phase, and in the aqueous phase, lauric acid-NBD appears as a product of ceramidase activity. We resolved lipids on TLC plates by using 1-butanol/acetic acid/water (3:1:1, v/v/v) and visualized by fluorescence with LAS-4000 (Fujifilm (λEx: 498 nm - λEm: 522 nm). We performed a semiquantitative evaluation of the spots with ImageJ.

2.9. Single-cell $[Ca^{2+}]_i$ measurements

We adjusted sperm loaded with Fluo-3AM to a concentration of 10×10^6. Cells were immobilized on poly-L-lysine-coated round coverslips, mounted on a chamber, and placed on the stage of an inverted microscope (Eclipse TE300 Nikon). We used a stroboscopic LED-based fluorescence illumination system to excite Fluo-3AM as described in [31]. We collected images (6 frames/minute) to perform fluorescent measurements. We used a filter with the following bandwidths: excitation 450-490 nm, dichroic mirror 505 nm, and emission 520-560 nm. We utilized a

Plan Fluor 40×/0.6 Nikon objective and collected images using NIS Element software (Nikon).

We microinjected C6-Cer to the bath solution (injection speed: 73 nl per second). We measured $[Ca^{2+}]_i$ after adding ionomycin to calibrate the maximal response. We performed fluorescence measurements as previously described in Suhaiman et al (2010). We processed fluorescence data offline utilizing the Image J. Raw intensity values imported were normalized using the following equations: a) (F/Fo) – 1. F is the fluorescence intensity at time t and Fo is the mean of F taken during the control period. All the results of (F/Fo)-1 were then graphed vs. time. %Δ(F/Fo)-1 is the difference between the fluorescence before stimulation and the maximal fluorescence obtained after the addition of C6-Cer. We graphed and analyzed with GraphPad Prism 5 data of three independent experiments.

2.10. Cell population calcium measurements

We loaded motile sperm (5-10 × 10^6 cells/ml) with the permeable dye (Fluo-3 AM, 2 μM). Washed cells were suspended in nominally calcium-free (~1 μM) medium (4 mM KCl, 10 mM Hepes-Na, 15 mM $NaHCO_3$, 120 mM NaCl, 5 mM D-glucose, 1 mM $MgCl_2$, 10 mM lactic acid, 1 mM sodium pyruvate, pH 7.4). We performed fluorescence measurements in cuvettes at 37°C. At the indicated times, 15 μM Pg, 10 μM C6, or 10 μM D-NMAPPD were added to the samples. We recorded Fluo-3 fluorescence

(λ_{Ex} = 505, λ_{Em} = 525nm) in an Aminco Bowman II spectrofluorometer.

In order to evaluate intracellular calcium movements, extracellular calcium was removed by adding 0.75 mM EGTA and 0.5 mM Ca^{2+} to the medium, resulting in a medium with [Ca^{2+}] ≤ 100 nM. Cells were loaded with Fluo-3AM, washed once, and suspended in buffer (0.75 mM EGTA, 0.5 mM Ca^{2+}, 120 mM NaCl, 10 mM Hepes-Na, 15 mM $NaHCO_3$, 4 mM KCl, 5 mM D-glucose, 1 mM $MgCl_2$, 10 mM lactic acid, 1 mM sodium pyruvate, pH 7.4). At the indicated times, Pg 15 μM, C6-Cer 10 μM, or 10 μM D-NMAPPD were added to the samples. Fluo-3 fluorescence was recorded as explained above.

A different set of experiments were performed testing calcium channel blockers in a media containing 2 mM Ca^{2+}. Cells were loaded with Fluo-3 AM and incubated for 10 min with 100 μM 2-APB, 1 μM XC, 1 mM YM-58483, 50 mM SKF-96365, 100 μM Verapamil, 20 nM Ruthenium red, or 1 μM NNC 55–0396 (NNC) previous to C6-Cer (10 μM) addition. We collected the data during 600 s at a frequency of 4 Hz (2 fps). We measured [Ca^{2+}]i after Triton X-100 (0.1%) addition to calibrate the maximal response. We performed five independent measurements by using different batches of sperm. For pairwise comparisons, we used the Tukey-Kramer post hoc test. We considered significant differences at the $p > 0.05$ level.

2.11. Statistical Analysis

One-way ANOVA was used to evaluate the data. We did not include in the analysis conditions used for data normalization (0% and 100%). We utilized the Dunnett post hoc test or Tukey-Kramer to compare the means with a control condition. When stated, we used a Student's t-test or Newman-Keuls Multiple Comparison Test. We considered significant differences at the $p > 0.05$ level.

3. Results

3.1. Enzymes of sphingolipid metabolism are present in human sperm

We previously demonstrated that S1P and SK1 participate in a signaling cascade leading to AR [20]. Given that the sperm is a terminal cell lacking protein synthesis and possess defined/limited metabolic pathways we decided to explore the presence of enzymes that metabolize the lipid precursors upstream this bioactive molecule. We resorted to Western blot and immunofluorescence assays to determine if enzymes involved in sphingolipid metabolism are present in human sperm.

Neutral sphingomyelinase2 (nSMase2) belongs to the family of sphingomyelinases that operate at neutral pH. They catalyze the removal of the phosphorylcholine group from sphingomyelin, producing ceramide [5]. To determine the presence of nSMase in human spermatozoa we performed a Western blot on 25×10^6

sperm extract obtained as described in Suhaiman et al (2010) [20]. Fig. 1A (whole sperm lysate) shows a protein band with a molecular mass of ~48kDa, matching with the MW described for nSMase, and a similar band in HeLa cells homogenate used as control (Fig. 1A, HeLa lane). We analyzed the nSMase localization by using indirect immunofluorescence. To distinguish between reacted and intact spermatozoa we double-labeled them with FITC-PSA (Fig. 1B, FITC-PSA and Cy3). Sperm showed a diffuse faint immunolabeling pattern in the head increasing the intensity in the midpiece in 80% of the cells (n=3 samples). This pattern is coincident with the presence of nSMases in the inner leaflet of the plasma membrane and the mitochondria of somatic cells [32]. Besides, a strong signal in the neck was found in 100% of stained cells.

We also evaluated the presence of ceramide synthase (CerS, Lass). This enzyme introduces the acyl chain to sphingoid bases, forming dihydroceramides and ceramides. We detected a main band of 46 kDa in both, whole sperm lysate and HeLa cells homogenate (Fig. 1C) and an additional nonspecific band of ~28 kDa, described by the manufacturer. Immunofluorescence showed strong staining in the acrosomal region (Fig. 1D).

These results demonstrated for the first time, that enzymes involved in the sphingolipid metabolism, like nSMase and CerS, were present in human sperm. These enzymes could be active and

affecting different functions during the span life of the male gamete. Even though the spermatozoon is a terminal cell lacking most organelles, its membranes are dynamic structures and undergo lipid remodeling during sperm maturation [33,34], capacitation [35,36], and the AR [37].

3.2. C6-Ceramide (C6-Cer) induces exocytosis of the acrosome in capacitated human sperm in a sphingosine 1-phosphate independent manner

Cross (2000) suggested that a sphingomyelin/ ceramide pathway plays a role during capacitation in human spermatozoa [18]. The preincubation of boar sperm with C2-ceramide enhanced the AR triggered by Ca^{2+}/ A23187 (calcium ionophore) [19]. Both results suggest the involvement of ceramide in the exocytosis of the acrosome granule. Nevertheless, these publications did not unveil the molecular mechanisms underlying ceramide and AR.

First, to find out if C6-Cer is implicated in the AR we challenged sperm with increasing concentrations of the lipid and evaluated the exocytic response. Exogenous C6-Cer triggered exocytosis in a dose-dependent manner (Fig. 2A). The number of cells that underwent AR augmented with the C6-Cer concentration achieving a maximum at 10 μM. Incubation of sperm with 10 μM C6-Cer elicits exocytosis as efficiently as progesterone (Pg, positive AR control for non permeabilized sperm) (Fig. 2A and B).

C6-Cer (10 μM) did not affect sperm viability assessed by using eosin to stain dead cells (control, 94.27% ± 1.10; 10 μM C6-Cer, 91.30% ± 0.93; mean ± S.E.), *n*=5 nor motility (control, 88.16% ± 3.88; 10 μM C6-Cer, 90.35% ± 2.45). In conclusion, C6-Cer triggers acrosomal exocytosis and do not affect sperm viability and motility.

Human spermatozoa are incapable to fertilize the egg after ejaculation. To gain fertilization competence, they require undergoing physiological changes during the passage through the female reproductive tract, named capacitation [38,39]. During capacitation, two critical events for fertilization occur the hyperactivated motility, an asymmetric and vigorous flagellar movement, and the capability to undergo the AR. To reveal the role of capacitation on C6-Cer-induced exocytosis, we mimicked this process *in vitro* (see Materials and Methods). We incubated sperm under capacitating (HTF media supplemented with 5 mg/ml BSA) or non-capacitating (HTF without BSA) conditions. Subsequently, we treated the cells with ceramide. Fig. 2B showed that only capacitated cells were able to respond to C6-Cer stimulus (compare grey, cap) and black (non-cap) bars, (C6). Further, we treated spermatozoa with 15 μM Pg to evaluate their capacitation status [40,41] (compare grey (cap) and black (non-cap) bars, Pg). Our results demonstrated that sperm required

capacitation to undergo the AR when challenged with C6-Cer involving this sphingolipid in a physiological pathway.

To determine if ceramide is involved in pathways already described for sperm exocytosis we incubated capacitated spermatozoa with 10 μM C6-Cer for 15 min. Then, the cells were treated with 15 μM Pg or 10 μM diacylglycerol (DAG). The exocytic response did not undergo a significant increase when DAG was sequentially added (Fig. 2D, C6→DAG) suggesting the possibility, that ceramide shares redundant signaling pathways with DAG rather than triggering a new one. However, progesterone showed a slight significantly increase (*$p<0.05$) when added after C6-Cer incubation (Fig. 2C, C6→Pg) suggesting that the physiological inducer and the lipid do not share completely the signaling pathway driving exocytosis, therefore, ceramide seems to potentiate sperm response to progesterone.

As mentioned previously, our laboratory demonstrated that exocytic stimuli trigger the sperm synthesis of S1P, which through its autocrine/paracrine action induces acrosomal exocytosis by binding to a Gi-coupled receptor. We hypothesized that ceramide, a precursor of this phosphorylated sphingolipid, could induce S1P synthesis (Fig. 2E) triggering the signaling cascade already described in Suhaiman et al. (2010)[20].

To test this prediction we preincubated capacitated human sperm with the sphingosine kinase inhibitor, SKI, before adding C6-Cer. SKI is a selective and potent inhibitor of SK [42]. As demonstrated, SKI inhibited the phorbol ester, PMA,-induced exocytosis suggesting that SK activity and S1P synthesis are required for the PMA-elicited cascade leading to AR [20] (Fig. 2F, SKI→PMA). However, SKI did not affect C6-Cer-induced AR in sperm (Fig. 2F, SKI→C6) suggesting that ceramide acute increase is not eliciting exocytosis through S1P synthesis.

3.3. C6-Cer addition induces physiological ultrastructural changes in the acrosome and triggers an exocytosis signaling cascade involving protein tyrosine phosphatase 1B and VAMP2

Upon sperm exocytosis stimulation, the acrosome swells. The outer acrosomal membrane (OAM) undergoes invaginations [43]. The edges of the invaginations get in touch with the plasma membrane forming tight appositions that become stable by trans SNARE complexes assembly. Cytosolic calcium increase triggers the opening and expansion of fusion pores in the site where the membranes are in contact. This process leads to the release of hybrid vesicles (half plasma membrane, half OAM) and the acrosomal content. In resting sperm, swollen acrosomes are barely observed by transmission electron microscopy (TEM) but the percentage of swelling increases in stimulated sperm that started

exocytosis. After that striking change, sperm lose their acrosome granules almost completely [44]. However, the equatorial region of the acrosome remains intact.

To dismiss the possibility that C6-Cer would be responsible for the sperm granule content release owing to membrane lipid alteration and consequently membrane destabilization, we first tested by TEM the changes in the sperm ultrastructure after challenging them with C6-Cer.

The percentage of swollen acrosomes was very low in resting sperm. Upon treatment with C6-Cer or the calcium ionophore, A23187, the percentage incremented to ~40% (Fig. 3A and B). Our data supply direct evidence that C6-Cer induces acrosome swelling, an intermediate stage required for sperm secretion dismissing the possibility of membrane disruption. The morphologies quantified in Fig. 3B are "intact" (non-swollen acrosomes); "swollen" (swollen acrosomes and waving with vesicles); and "reacted" (lost acrosomes).

To gain further understanding into the molecular mechanism through which C6-Cer triggers the AR we tested if the ceramide is activating a pathway involving the activity of protein tyrosine phosphatase 1B (PTP1B). Zarelli et al (2009) identified that during sperm exocytosis, after Rab3A activation, PTP1B is dephosphorylating NSF (N-ethylmaleimide-sensitive factor). This produces the disassembly of fusion-incompetent cis SNAREs

(SNAP receptor) complexes, the main arrangement in resting sperm, into reactive monomeric synaptobrevin2, SNAP-25, and syntaxin1 [25]. Therefore, PTP1B could be dephosphorylating NSF and eliciting the disassembly of SNARE complex required for sperm secretion to proceed (Fig. 3C). We resorted to the photosensitive PTP Inhibitor I to elucidate if C6-Cer effect is governed by NSF tyrosine dephosphorylation during the AR triggering the canonical pathway of acrosome exocytosis. The inhibitor binds covalently to the catalytic domain of PTP1B, disrupting its enzymatic activity. U.V. light irradiation reverses the inhibition.

As shown in Fig. 3D, PTP inhibitor I inhibits significantly Pg-induced AR (PTPi→Pg). The effect was reversed by U.V. light irradiation (PTPi→Pg→hν). A similar result was observed when we used C6-Cer as a stimulus. The PTP1B blocker inhibited the C6-Cer-induced exocytosis and it was reversed by U.V. light irradiation (Fig. 3D, PTPi→C6; PTPi→C6→hν) meaning that both Pg and C6-Cer converged in a cascade that activates PTP1B and required the phosphatase for the AR to proceed.

Controls using the PTP Inhibitor I with or without U.V. light exposure demonstrated that they differ significantly from PTPi→Pg/C6→hν indicating that the PTP inhibitor I is not able to induce exocytosis when added alone (Fig. 3D).

As described by De Blas et al (2005), calcium triggers complex signaling in human sperm that finally disassembles neurotoxin-resistant cis and provokes the assembly of toxin-sensitive loose trans-SNARE complexes necessary for AR [45]. We decided to assess if C6-Cer-induced secretion needs functional SNAREs (Fig. 3E). Given that, sperm are unable to synthesize proteins we find a big hindrance to applying classic molecular and cell biology approaches. In past publications, we used the light chains of botulinum or tetanus neurotoxins in permeabilized spermatozoa to avoid calcium- or different stimuli-induced exocytosis [26,43]. Here, we developed a novel tool to overcome this limitation: delivery of permeant proteins. This grants an accurate understanding of sophisticated pathways induced by known AR inducers given that it allows membrane translocation to intracellular compartments. We took advantage of a recombinant protein developed at the laboratory. We used a recombinant Te-Tx conjugated with a cell-penetrating peptide. To evaluate our hypothesis, we incubated sperm with the permeant light chain of Te-Tx to cleave VAMP2 before C6-Cer addition. The treatment inhibited significantly both C6-Cer and A23187 calcium ionophore-induced exocytosis (Fig. 3E). This result not only indicates that the ceramide leads to the fusion machinery activation, but it also discards that the sphingolipid would be inducing the AR through membrane disruption.

These novel experimental approaches, along with TEM assays results, confirm that C6-Cer is triggering a regular membrane fusion rather than destabilizing membranes or working through a still unknown mechanism. Further, progesterone converges with ceramide, at least, at the final stages of the membrane fusion.

3.4. Ceramidases are present and active in human sperm and endogenous ceramide increase induces acrosomal exocytosis

Ceramidases hydrolyze the fatty acyl groups from ceramides. Based on their optima pH activity they are classified in three different families: acid, neutral, and alkaline. Probing human sperm extracts with the anti-nCDase (neutral ceramidase) (Fig. 4A) on Western blots showed a protein band of ~84 kDa that matches with the MW of the enzyme described in the literature and with the band found in mouse testis homogenate used as control (Fig. 5A, m-testis lane). To determine nCDase localization in human sperm, immunofluorescence analysis with the same antibodies was carried out (Fig. 4B). nCDase was localized to the acrosomal region and the midpiece of the flagellum in 70 % of the sperm (n=5 samples). The acrosomal staining is lost when sperm are reacted (data not shown).

Ceramide is converted by ceramidase to sphingosine and fatty acid. To evaluate if ceramidases are active in sperm and if their activity is affected by the potent ceramidase inhibitor, D-NMAPPD, we adapted a method of thin-layer chromatography

described by Tada et al (2010) to sperm [30]. Sperm were loaded with fluorescent ceramide (4-nitrobenzo-2-oxa-1,3-diazole–labeled C12-ceramide, NBD-ceramide). Subsequently, we separated the ceramide metabolites by lipophilicity and analyzed the levels of lauric acid in the aqueous phase, which is the product of ceramidase activity.

This enzyme activity is upregulated by Ca^{2+} [46]. Considering this property, we decided to increase sperm intracellular calcium with an ionophore, A23187, and subsequently, we evaluated ceramidase activity in the presence or not of D-NMAPPD. As shown in Fig. 4C and D there is an important basal activity of the enzyme in human sperm and a calcium increase induces a rise in ceramidase activity measured by an augment of lauric acid in the aqueous phase. This increment was inhibited by D-NMAPPD. In conclusion, calcium-induced ceramidase activity decreases when sperm are in the presence of the enzyme inhibitor.

Sperm membranes have an atypical lipid composition. The presence of sphingomyelins and ceramides containing high levels of long-chain and very-long-chain polyunsaturated fatty acids is a characteristic of mammalian sperm membranes [47]. During capacitation and AR in rat sperm, significant biochemical changes in these lipid species take place [48,49,50].

Given that, the experiments shown in Fig. 2 and 3 were done by adding exogenous C6-Cer and the fatty acid composition of sperm

sphingolipids are very unique we asked if endogenous ceramides increase achieve acrosome release as the C6-Cer did. As demonstrated in Fig. 4A-D, ceramidases are not only present in human sperm but active. Then, we incubated spermatozoa with increasing concentrations of the ceramidase inhibitor, D-NMAPPD, to increase endogenous ceramide levels [51]. We found that D-NMAPPD induces exocytosis as C6-Cer did in a dose- dependent fashion (Fig. 4E) achieving a maximum at 25 μM. Given that the acrosomal exocytosis index between 10 and 25 μM is not significantly different we chose 10 μM to perform the experiments. By using eosin, we determined 92% of cell viability at this concentration (data not shown). D-NMAPPD induced the AR to the same extent as progesterone. The last result suggests that the endogenous ceramide exerts the same effect on the AR that the exogenous one implying that the sphingolipid is involved in physiological molecular mechanisms of acrosome secretion.

3.5. Ceramide increase induces intracellular calcium rise in live human sperm

By scrutinizing the literature for information, we conclude that the ceramide effect on cell calcium mobilization is controversial. In some cellular types, ceramide diminishes intracellular calcium by inhibiting extracellular calcium entry [9,52]. In other cell types, it provokes a cytosolic calcium rise by inducing release from

intracellular reservoirs and opening of a store-operated calcium channel [11,12,53]. Sperm possess particular Ca^{2+} stores, like the acrosome, the redundant nuclear envelope (RNE), and the mitochondria. The effect of ceramide on spermatozoa's intracellular calcium concentration is largely unknown. To directly assess the effect of C6-Cer addition on $[Ca^{2+}]i$ in live sperm, we loaded the cells with the permeant Ca^{2+} indicator Fluo-3 AM dye. Then, we measured Ca^{2+} changes in single-cell experiments and cell population. We used human sperm media (HTF) with 2 mM $CaCl_2$ final. We noticed that 46% of the cells suffered an $[Ca^{2+}]i$ increase when challenged with C6-Cer during the experiment. Single-cell $[Ca^{2+}]i$ images of spermatozoa reacting to 10 μM C6-Cer treatment are shown in Fig. 5A. When we repeated experiments with other sperm batches, comparable results were obtained. The percentage of changes in fluorescence after C6-Cer addition was represented in Fig. 5B. Summarizing, these results revealed that exogenous ceramide augments $[Ca^{2+}]i$ in the sperm head and neck regions.

To analyze the behavior of the sperm population, human sperm bathed in the same media and loaded with Fluo-3 AM were treated with 10 μM C6-Cer. Cells responded to C6-Cer addition (Fig. 5D) with a transient calcium rise similar to that induced by progesterone under the same conditions (Fig. 5C). Incubation with the ceramidase inhibitor, D-NMAPPD, induced a calcium rise of

a similar magnitude of that observed by adding ceramide (Fig. 5E). These data altogether suggest that, under identical treatments where exogenous and endogenous ceramides elicit exocytosis in sperm, they increase the cytosolic calcium concentration (Fig. 5F) leading to the idea that the sphingolipid is either activating a calcium channel or a signaling cascade involving a calcium channel.

3.6. Ceramide increase promotes calcium mobilization from internal stores but requires extracellular calcium influx to accomplish acrosome release

We asked if, C6-Cer-triggered intracellular calcium increase needs extracellular Ca^{2+} entry like some physiological inducers of the AR. To solve this issue, we treated capacitated sperm with HTF containing 0.75 mM EGTA to chelate extracellular calcium leaving the media with a $[Ca^{2+}] \leq 100$ nM. Then, cells were loaded with the calcium probe Fluo-3AM before adding the C6-Cer stimulus. As predicted, we observed that the absence of calcium in the extracellular media avoided $[Ca^{2+}]$i increase when Pg was added (Fig. 6A). On the contrary, sperm responded to C6-Cer or the ceramidase inhibitor (D-NMAPPD) treatments with an increase in calcium concentration (Fig. 6B and C). We obtained equivalent results when we replicate the experiment with many sperm batches. Results from Fig. 5 and 6 were summarized and compared in Fig. 6D. Based on these data, we reasoned that both

endogenous and exogenous ceramides increase, induce an increment in sperm $[Ca^{2+}]i$ by promoting calcium efflux from internal reservoirs.

Next, we asked whether intracellular calcium increase induced by ceramides, in the lack of extracellular calcium, was enough to trigger the AR. To assess this issue, we resorted to exocytosis assays. By performing functional assays, under the same conditions as the calcium measurements described above, we demonstrated that EGTA presence in the media ($[Ca^{2+}] \leq 100nM$) abolished the exocytic effect of exogenous and endogenous ceramide (Fig. 6E, C6 and D-NMPAAD respectively). These results suggest that calcium entry is needed for ceramide-elicited AR. Progesterone-triggered secretion relies on calcium influx as previously demonstrated [23] and Fig. 6E. We used another approach to test the requirement of extracellular calcium for ceramide-elicited exocytosis. Human sperm suspended in HTF media (see Methods) were incubated in 5 mM BAPTA for 15 min. After that, C6-Cer was added. As shown in Fig. 6F, BAPTA→C6, the treatment was enough to abolish the sperm granule exocytosis. The last results suggest that Ca^{2+} influx from the media is required for C6-Cer-induced AR.

In conclusion, ceramide rise mobilizes calcium from internal stores inducing a cytosolic calcium increase but requires extracellular calcium influx to release the acrosome content. This

is coincident with the known mechanism leading to acrosome exocytosis where extracellular calcium entry, through voltage-operated Ca^{2+} channels (VOCCs) and store-operated Ca^{2+} channels (SOCCs), is an essential requirement [54].

3.7. C6-Cer-induced calcium mobilization and acrosome exocytosis involve the activation of ryanodine receptors and extracellular calcium influx through CatSper and SOCCs

Zona pellucida glycoproteins (ZP3, ZP4) and progesterone induce human sperm exocytosis. The current hypothesis is that upon activation, the opening of VOCCs in the plasma membrane provokes a transient rise in $[Ca^{2+}]_i$ [55]. This Ca^{2+} increase activates a release of calcium from internal stores. The calcium loss from these reservoirs triggers the opening of SOCCs producing a sustained Ca^{2+} augment that starts the AR [56,57]. In spite of the key role that calcium channels play in the AR, their identity and regulation are not fully understood.

To elucidate which calcium channel/s are involved in C6-Cer-induced ion mobilization human sperm bathed in HTF medium with 2 mM $CaCl_2$ and loaded with Fluo-3AM were treated with specific calcium channels blockers and the changes in intracellular calcium concentration were measured in sperm population after adding C6-Cer.

The arylalkylamine Ca^{2+} antagonist, Verapamil, mainly inhibits the L-type high voltage-activated Ca^{2+} currents [56].

Preincubation of sperm with 100 μM verapamil diminished partially but not significantly (Fig. 7H) the calcium-increase caused by ceramide addition Fig. 7A, light blue compared to the red curve (control, which represents the result obtained with C6-Cer alone).

Given that we demonstrated that both exogenous and endogenous ceramide promotes calcium mobilization from internal stores (Fig. 6) we treated sperm with specific store calcium channel blockers. To determine if ceramide-elicited calcium rise requires calcium efflux through IP_3-sensitive calcium channels we incubated sperm with specific inhibitors (2-APB and xestospongin C, XC). Nor 2-APB neither XC was able to block C6-Cer-triggered calcium mobilization (Fig. 7B and C, 2-APB, green and XC, yellow) suggesting that ceramide does not lead to calcium efflux from the stores through IP_3-dependent calcium channels, at least during the time the measurements where done (100 sec). Profuse evidence exists for a functional RNE Ca^{2+} store in human spermatozoa that corresponds pharmacologically to a ryanodine receptor gated store [58,59,60]. Ryanodine receptors (RyRs) are present in spermatogenic cells, that express transcripts for different RyR isoforms (For a review see Darszon et al (2011) [56]). Zhou et al, (2013)[61] also described the presence of RyRs in mouse mature sperm. The increment in $[Ca^{2+}]i$ induced by ceramide was abolished by the preincubation of cells with the RyR blocker,

ruthenium red (RR, 20 nM), indicating that the calcium store involved primarily and early in this pathway could be the RNE (Fig. 7D).

Even though ceramide induces $[Ca^{2+}]_i$ increase in a media without calcium we decided to investigate if plasma membrane channels were contributing to $[Ca^{2+}]_i$ rise.

To determine if SOCCs opening are necessary for the C6-Cer-stimulated calcium increase we resorted to specific inhibitors of aforementioned channels: YM-58483 [62] or SKF-96365 [63,64]. Both, 1 μM YM-58483 and 50 μM SKF-96365 impeded C6-Cer-induced calcium increase (Fig. 7E, SKF, blue and f, YM, brown) indicating that Ca^{2+} entry through SOCCs is involved in the calcium rise elicited by ceramide. However, a slight intracellular calcium increase is observed when the SOCCs inhibitors are present likely due to calcium release from internal stores (RyR). The CatSper (calcium channel of sperm) is crucial for male fertility and its activity is modulated by progesterone and other endogenous steroids [65]. To evaluate whether C6-Cer activated CatSper, we incubated sperm with a channel inhibitor: NNC 55–0396 (NNC, 1 μM) [66], before ceramide addition. NNC inhibited C6-Cer-elicited calcium increase indicating that ceramide is a lipid capable of activating CatSper (Fig. 7G). Given that the experiments showed in Fig. 6A, B and, C were performed in the absence of extracellular calcium we should consider that CatSper,

under this condition, can transport monovalent cations like Na^+ and/or K^+ [67], inducing changes in membrane polarization which in turn elicits numerous and diverse biological effects. Here, CatSper and RyR blockers abolished ceramide-induced calcium rise. Altogether, these results and those observed in Fig. 6, allow us to hypothesize that the opening of both channels occurs at the same time and require each other to be active, acting in concert to mobilize calcium.

Fig. 7H shows the increase (ΔF) in fluorescence after treatments described above and expressed as (F/F0)-1 ((maximum fluorescence intensity/initial fluorescence)-1). Mean±S.E. of five experiments are depicted in bars and data compared to the C6-Cer condition.

In conclusion, VOCCs and IP_3-sensitive calcium channels blockers do not affect the intracellular calcium increase triggered by ceramide during the first 100 sec of the treatment. On the other hand, RyR, CatSper, and SOCCs inhibitors abolished ceramide-induced calcium rise at a very early stage.

This is consistent with the idea that ceramide drives calcium mobilization from internal stores, in this case, RNE, and depletion of the ion reservoir could activate SOCCs opening. Because not all the calcium fluctuations occurring in sperm drives to the acrosome exocytosis, we asked whether ceramide required the activation of RyR, CatSper, and SOCCs to accomplish the AR. To

solve this issue, we resorted to exocytosis assays using the same specific calcium channel blockers and the loss of the acrosome as a readout. As showed in Fig. 7I the VOCCs blocker, verapamil, did not inhibit C6-Cer-induced acrosome exocytosis as well as it did not inhibit the calcium increase caused by ceramide. This result suggests that VOCCs are not involved in ceramide-induced exocytosis. On the other hand, C6-Cer-triggered AR was significantly inhibited by store channels (XC, 2-APB, and RR) and SOCCs (SKF and YM) blockers indicating that these channels are required for the C6-Cer-induced acrosome exocytosis to proceed. It is important to highlight that calcium increase during the first seconds after the lipid addition is CatSper and RyR dependent but IP_3-sensitive calcium channels independent. These functional results support the hypothesis suggesting that ceramide drives CatSper activation and calcium mobilization from internal stores at the same time. Depletion of the reservoirs activates SOCCs opening and signaling leading to membrane fusion.

4. Discussion

Ceramide plays critical roles in many cellular processes including membrane fusion [13]. Ceramide effect on exocytosis is highly controversial and the downstream effector(s) of the molecule in this biological process is largely unknown.

In sperm, lipid turnover occurs during capacitation and exocytosis of the acrosome [26,37,49,68]. Specifically, the highest Cer:SM ratio was found after AR termination in rat sperm and the amount of SM→Cer shift correlates with the extent of the AR. The synthesis of Cer in the spermatozoa may be an early step in the physiological changes leading to fertilization [47]. Even that this lipid turnover has been demonstrated in the sperm of different species there are very few data about the enzymes involved in this process. Here, we identified for the first time the presence and location of sphingolipid metabolism enzymes in human sperm.

We found that a neutral sphingomyelinase is present in human sperm. Concerning to male gametes of other species, a highly active nSMase was found in ram sperm membranes [69]. Furland et al. (2007) suggest the presence of an isoform of neutral sphingomyelinase in rat and bull epididymal spermatozoa [47]. Further, Wang et al. [70] described the human spermatozoa proteome reporting the presence of different isoforms of neutral and acid sphingomyelinases in the male gametes.

We also identified a neutral ceramidase in human spermatozoa. Further, we demonstrated a basal and regulated ceramidase activity in the gamete. Our results highlight the importance of sphingolipids continuous remodeling, which seems to be essential for sperm function. In support of our results, the inhibition of an

alkaline ceramidase activity in boar sperm enhances A23187-induced acrosome reaction [19].

The fact that we found a ceramide synthase (CerS, Lass), did not mean that ceramides could be synthesized de novo in human sperm but we cannot discard the idea.

We hypothesize that human sperm requires a precise equilibrium between SM, Cer, sphingosine, and S1P depending on its maturation state, capacitation, or during the acrosome reaction. This equilibrium is not only regulated by sphingolipid metabolism enzymes but also by the external media that changes while the spermatozoa transit across the female genital tract before fertilization.

Here, we offer profuse evidence indicating the occurrence of a novel pathway triggered by C6-Cer in human sperm exocytosis. The lipid triggers the AR in a concentration-dependent manner in capacitated human sperm reaching a maximum at 10 μM. Even though, we increased ceramide concentration up to 25 μM the percentage of acrosome secretion did not change significantly. However, non-capacitated sperm were not responsive to C6-Cer suggesting that lipid remodeling and/or biochemical changes during capacitation are crucial for ceramide-induced AR.

Notably, we observed that ceramide potentiates progesterone-induced exocytosis in agreement with results published by Cross (2000) [18]. Progesterone signaling cascade to exocytosis it is not

well defined yet, and these results could be suggesting different pathways for progesterone and ceramide. Although, when we analyzed the molecular mechanism induced by the lipid, we found that it is activating the CatSper channel (Fig. 7) just as progesterone does [71]. This is a very early event in the signaling cascade driving the AR. Therefore, it makes sense that ceramide activates CatSper when incubated with gametes, and another batch of cells responds to progesterone addition with a calcium wave through this channel, increasing the number of responsive cells. We postulate that the mechanism of CatSper activation for both inducers could be different, considering the ability of ceramides to activate voltage-dependent channels and the interaction demonstrated for progesterone with its receptor. Both cascades converge on DAG. We hypothesize that the signaling pathway induced by progesterone involves more actors on a stage than the delimited pathway triggered by DAG, which is directly involved in IP_3-sensitive calcium channels opening [68].

Even though our laboratory demonstrated that S1P triggers the AR in human sperm [20], ceramide's rise does not induce the exocytosis of the acrosome by a displacement of the chemical equilibrium to the direction of this bioactive sphingolipid. On the contrary, C6-Cer addition induce sperm exocytosis even in the presence of the sphingosine kinase inhibitor that abolished S1P production. These results lead us to conclude that although S1P is

a pathway necessary for the exocytosis an acute ceramide increase promotes an alternative signaling cascade.

It is possible that both, endogenous and exogenous ceramide increase, could affect the biophysical properties of the membranes. Numerous lines of evidence point toward the requirement of a localized asymmetric generation of fusogenic lipids for the onset of fusion. Such a ‘‘hot spot’’ can arise if the synthesis of ceramide, is fast enough to overcome the diffusion of these lipids along the bilayer. The small polar head group of ceramide (cone-shaped lipid) generates an inward curvature of the monolayer where it locates (‘‘negative curvature’’). Holopainen et al. (2000)[72] observed ceramide’s ability to segregate into patches leading to membrane invagination. Even though we do not discard this possibility, our results constitute a strong piece of evidence indicating that ceramide triggers a signaling cascade that drives acrosomal exocytosis. Supporting this, it is necessary to highlight that, a non-linear relationship between C6-Cer concentration and AR was observed and that the addition of an AR inducer, like DAG, to C6-Cer preincubated sperm, did not induce a significant increase in exocytosis. Last but not least, the analysis of the sperm morphology by TEM after ceramide treatment showed that the lipid-induced swelling during exocytosis shares similar characteristics of that provoked by different AR inducers [43,44]. These results suggest that ceramide

is not inducing membrane destabilization even though biophysical and biochemical properties of the lipid could drive a joint action to reach the exocytosis.

Further, we confirmed that C6-Cer was triggering a cascade that activates PTP1B and required the phosphatase for SNARE disassembly and consequently for exocytosis. Another contribution of our work is that the pathway triggered by progesterone, which is not fully elucidated yet, requires PTP1B activity for acrosome secretion as ceramide does. These findings provide new molecules involved in the biochemical cascade that leads to progesterone-induced exocytosis. We showed that C6-Cer requires active fusion proteins by using a novel tool developed at the laboratory to cleave VAMP2. Taken together, our results indicate that both ceramide and progesterone-elicited exocytosis require fusion competent SNAREs complexes to occur.

The AR stimuli produce an intracellular multicomponent calcium increase [3,73]. Ceramide is not an exception and promoted calcium mobilization from internal stores. Here, we presented pharmacological evidence indicating that RyRs are activated after ceramide treatment. Nevertheless, this intracellular calcium mobilization is not enough to elicit exocytosis. It required a calcium entry through CatSper and SOCCs to release the granule content. Our results demonstrate that IP_3-dependent calcium channels are not implicated in primary ceramide-triggered

calcium rise but necessary for AR to occur. Progesterone activates a Ca^{2+} influx through CatSper channels present at the midpiece of the flagella in human sperm [66,74]. Furthermore, channel activity is required for male fertility. Several authors described an anterograde wave of Ca^{2+} when sperm were challenged with soluble ZP [75] [76]. This lead to the hypothesis that a Ca^{2+} reservoir located in sperm's neck may be associated with the acrosome secretion. We propose that C6-Cer initiates a cascade, at least in part, by activating CatSper and RyR calcium channels in an early stage and could be generating a calcium current towards the head. The signaling cascade we postulate matches with the neutral sphingomyelinase localization at the sperm midpiece.

Even we demonstrated that ceramide is mobilizing calcium from internal stores, results depicted in Fig. 7 by using different channel blockers, showed that intracellular calcium rise requires the activity of channels from intracellular reservoirs (RyR) and plasma membrane (SOCCs and Catsper).

Does the absence of calcium increase in Fig. 7D when RyRs are inhibited, argue against CatSper function in ceramide-induced calcium rise? We hypothesize that, at the early stages of the AR, ceramide elicits simultaneous CatSper and RyR activation that guarantees the ceramide-induced calcium signaling. By examining the literature, we found that in cardiac myocytes

incubated in a media without calcium, membrane depolarization is induced by sodium, triggering the calcium efflux from RyR [77]. Further, in skeletal muscle cells, ryanodine sensitivity to Ca^{2+} release augments by membrane depolarization [78]. CatSper is a pH-sensitive, voltage-dependent ion channel that regulates the influx of positively charged calcium ions into spermatozoa [66]. CatSper can allow passage of monovalent cations (e.g. Na^{+}) when divalent cations are not present in the extracellular media. We propose that in the absence of calcium, (Fig. 6A, B, and C), Na^{+} entry through CatSper causes membrane depolarization, eliciting calcium release from ryanodine-sensitive internal stores. SOCCs may be also supporting this process due to Na^{+} entry in the absence of calcium [67]. Results showed in Fig 7D and G, indicate that the rapid $[Ca^{2+}]_i$ rise produced by ceramide relies on both CatSper and RyR joint activities. Each channel could not work if the other one is inhibited. Given that we are the first group describing this effect, the mechanism by which ceramide activates CatSper is unknown. We found literature showing that the sphingolipid regulates voltage-dependent calcium channel activity in pinealocytes and GH3 cells [79,80]. Ceramide also affects voltage-dependent K^{+} channels by the formation of membrane platforms [81]. Interestingly, ceramide mediates Src activation in hippocampal neurons and Src is a crucial kinase that regulates hyperpolarization through SLO3 potassium channel in sperm [82].

Therefore, ceramide could be regulating CatSper by different mechanisms.

What about SOCCs? Fig. 7E and F show a small intracellular calcium increase when ceramide is added in the presence of SOCCs inhibitors. We reasoned that this calcium rise is probably coming from RyR and CatSper opening.

Numakawa et al. demonstrated that in cultured developing cerebellar neurons, NGF provokes a fast release of glutamate by activation of the plasma membrane neutral sphingomyelinase. The consequently ceramide's synthesis, which induces Ca^{2+} release through the RyR, emptying this store, causes the opening of SOCCs triggering the neurotransmitter release [13]. These results support the pathway we describe here for human sperm secretion. Further, NGF and its receptors are expressed in accessory reproductive organs, epididymal sperm, and the testis. NGF induces the AR, in a dose- and time-dependent fashion [83]. This effect has been observed in different species including human sperm [84]. Probably our results describe the molecular mechanism by which NGF exerts its effect on sperm exocytosis.

Based on the results presented here, we established a working model illustrated in Fig. 8. Progesterone and/or ceramide activate CatSper channels in human sperm, generating $[Ca^{2+}]i$ increase at the midpiece. Progesterone binds to its membrane receptor activating the CatSper by a known mechanism [66,85,86]. In

human sperm, 2-arachidonoylglycerol (2-AG) is an endogenous inhibitor of CatSper. Progesterone activates the α/β hydrolase domain-containing protein 2 (ABHD2) [71], which cleaves 2-AG into glycerol and arachidonic acid (AA). Arachidonic acid and polyunsaturated fatty acids, especially abundant in sperm, regulate n-SMase activity (for a review see [87]). Therefore, a physiological stimulus like progesterone could increase endogenous ceramide.

Exogenous ceramide can activate n-SMase *in vivo*, which hydrolyzes SM producing endogenous ceramide [88]. Therefore, many stimuli could be increasing ceramide concentration.

Therefore, ceramide-elicited $[Ca^{2+}]_i$ increase during the first 40 sec occurs, at least, by three mechanisms, (i) influx through CatSper channels, (ii) efflux through RyR from RNE, and (iii) an early SOCCs entry. The calcium rise could be triggering a cascade that activates PLC, which hydrolyzes PIP_2 to produce IP_3 and DAG. The activation of IP_3-dependent calcium channels and the additional emptying of stores, which are refilled continuously by a Ca^{2+}-ATPase pump[89], would consequently stimulate the permanent opening of SOCCs inducing a sustained calcium increase that triggers the signaling pathway leading to exocytosis of the acrosome granule. According to our results, in this cascade progesterone and ceramide converge in PTP1B activation that

could be dephosphorylating NSF and driving SNARE complex disassembly for sperm exocytosis to occur.

Both, our results and lipids characterized as modulators of sperm exocytosis probably implies a link between the ceramide and progesterone signaling cascades. On the contrary, we already demonstrated that the S1P is not a sphingolipid required for progesterone-induced sperm exocytosis [20].

Here, we present the first evidence demonstrating that ceramide promotes the human sperm exocytosis. Our results, accomplished with specific tools and different strategies, are consequent with the concept that ceramide fits like a key component in the molecular cascade puzzle leading to acrosomal exocytosis.

5. Conclusions

This study supplies strong evidence demonstrating the existence of decisive pathways regulated by ceramide during sperm exocytosis. Our results shed light on the controversial participation of a multitasking lipid in a signaling pathway driving exocytosis.

Ceramide increase induces the exocytosis of the sperm secretory granule and potentiates progesterone effect. We present profuse evidence indicating that ceramide is not inducing membrane destabilization but a physiological signaling pathway. Namely, (i) Acrosome ultrastructural changes, analyzed by TEM after ceramide addition, are similar to that observed in progesterone or

A23187 treated sperm; (ii) Ceramide-induced AR occurs only in capacitated sperm; (iii) The phosphatase PTP1B and the membrane fusion protein VAMP2, known important participants in exocytosis, are required for ceramide-elicited membrane fusion; (iv) The sphingolipid shares some molecular mechanisms with the physiological inducer progesterone and the lipid DAG.

Notably, the $[Ca^{2+}]_i$ calcium increase induced by ceramide at the very early stages of the acrosomal exocytosis implies influx of the ion through channels such as CatSper and SOC, and efflux through RyR from RNE. Interestingly, this first calcium wave does not rely on classical VOCCs activation as described in the canonical pathway for acrosome granule exocytosis. Calcium mobilization and the fusion machinery assemblage merge to achieve the fusion of the acrosomal granule with the plasma membrane.

Given that, the sphingolipid pathway is present and active in the male gamete; our results confirm that human sperm requires a precise equilibrium between different sphingolipids to accomplish fertilization. We are aware that the female genital tract is also regulating this equilibrium before fertilization.

Importantly, here we characterize new components of the signaling pathway through which the progesterone accomplishes the acrosome exocytosis by the requirement of the phosphatase PTP1B activity. This is a significant contribution to the biology of

reproduction field. Our findings indicate that progesterone and ceramide-elicited exocytosis joint in the requirement of functional SNAREs to occur.

Our research benefits the exocytosis field highlighting the notion that secretion can be regulated by ceramide concentration in membranes. This concept will contribute to the knowledge unveiling how exocytosis could be regulated in specialized secretory cells.

Consent for publication

All authors read and are consent for the publication of the manuscript.

Competing interests

The authors declare that they have no competing interests.

Funding

This work was supported by grants from Agencia Nacional de Promoción Científica y Tecnológica (PICT-2015-1222, Argentina), CONICET (PIP Nº 11220120100267, Argentina), and SECTyP-Universidad Nacional de Cuyo (grant number 06/J467, Argentina) to SAB.

Authors' contributions

CCV carried out the majority of the AR assays, enzyme activity assays, electron microscopy experiments, calcium measurements, analyzed the data, and performed the statistical analysis. LS performed functional assays, composed the Figures, and

participated in the writing. MAP developed the recombinant Te-Tx conjugated with a cell-penetrating peptide, carried out functional assays and analyzed the data. GADB carried out the calcium imaging studies and analyzed the data. SAB conceived of the research, designed, coordinated the work, and wrote the manuscript. All authors read and approved the final manuscript.

Acknowledgements

The authors thank E. Bocanegra and R. Militello, PhD for excellent technical assistance. We also thank A. Morales, PhD and P. López, MS from the STAN: ST3371 of TEM and SEM samples preparation, IHEM-CONICET-UNCuyo.

We are also grateful to Dr. Mayorga for useful discussions and for substantial contributions to interpretation of data. Dr. Mayorga also revised this manuscript critically for important intellectual content.

References

[1] A.I. Yudin, W. Gottlieb, S. Meizel, Ultrastructural studies of the early events of the human sperm acrosome reaction as initiated by human follicular fluid, Gamete Res. 20 (1988) 11-24.

[2] J.E. Flechon, R.A. Harrison, B. Flechon, J. Escaig, Membrane fusion events in the Ca2+/ionophore-induced acrosome reaction of ram spermatozoa, J Cell Sci 81 (1986) 43-63.

[3] A. Darszon, J.J. Acevedo, B.E. Galindo, E.O. Hernandez-Gonzalez, T. Nishigaki, C.L. Trevino, C. Wood, C. Beltran, Sperm channel diversity and functional multiplicity, Reproduction. 131 (2006) 977-988.

[4] N. Bartke, Y.A. Hannun, Bioactive sphingolipids: metabolism and function, J Lipid Res 50 Suppl (2009) S91-96.

[5] Y.A. Hannun, L.M. Obeid, Principles of bioactive lipid signalling: lessons from sphingolipids, Nat.Rev.Mol.Cell Biol. 9 (2008) 139-150.

[6] A. Gomez-Munoz, N. Presa, A. Gomez-Larrauri, I.G. Rivera, M. Trueba, M. Ordonez, Control of inflammatory responses by ceramide, sphingosine 1-phosphate and ceramide 1-phosphate, Prog Lipid Res 61 (2016) 51-62.

[7] A. Alonso, F.M. Goni, The Physical Properties of Ceramides in Membranes, Annu Rev Biophys 47 (2018) 633-654.

[8] N.A. Bourbon, L. Sandirasegarane, M. Kester, Ceramide-induced inhibition of Akt is mediated through protein kinase Czeta: implications for growth arrest, J Biol Chem 277 (2002) 3286-3292.

[9] C.L. Chik, B. Li, T. Negishi, E. Karpinski, A.K. Ho, Ceramide inhibits L-type calcium channel currents in rat pinealocytes, Endocrinology 140 (1999) 5682-5690.

[10] R. Mihai, T. Lai, G. Schofield, J.R. Farndon, C2-Ceramide increases cytoplasmic calcium concentrations in human parathyroid cells, Biochem Biophys Res Commun 268 (2000) 636-641.

[11] E. Kobrinsky, A.I. Spielman, S. Rosenzweig, A.R. Marks, Ceramide triggers intracellular calcium release via the IP(3) receptor in Xenopus laevis oocytes, Am J Physiol 277 (1999) C665-672.

[12] C. Colina, A. Flores, H. Rojas, A. Acosta, C. Castillo, R. Garrido Mdel, A. Israel, R. DiPolo, G. Benaim, Ceramide increase cytoplasmic Ca2+ concentration in Jurkat T cells by liberation of calcium from intracellular stores and activation of a store-operated calcium channel, Arch Biochem Biophys 436 (2005) 333-345.

[13] T. Numakawa, H. Nakayama, S. Suzuki, T. Kubo, F. Nara, Y. Numakawa, D. Yokomaku, T. Araki, T. Ishimoto, A. Ogura, T. Taguchi, Nerve growth factor-induced glutamate release is via p75 receptor, ceramide, and Ca(2+) from ryanodine receptor in developing cerebellar neurons, J Biol Chem 278 (2003) 41259-41269.

[14] A. Abousalham, C. Liossis, L. O'Brien, D.N. Brindley, Cell-permeable ceramides prevent the activation of phospholipase D by ADP-ribosylation factor and RhoA, J.Biol.Chem. 272 (1997) 1069-1075.

[15] P.J. Mansfield, S.S. Carey, V. Hinkovska-Galcheva, J.A. Shayman, L.A. Boxer, Ceramide inhibition of phospholipase D and its relationship to RhoA and ARF1 translocation in GTP gamma S-stimulated polymorphonuclear leukocytes, Blood 103 (2004) 2363-2368.

[16] N. Tang, W.Y. Ong, E.M. Zhang, P. Chen, J.F. Yeo, Differential effects of ceramide species on exocytosis in rat PC12 cells, Exp.Brain Res. 183 (2007) 241-247.

[17] J.E. Ji, S.K. Kim, K.H. Ahn, J.M. Choi, S.Y. Jung, K.M. Jung, H.J. Jeon, D.K. Kim, Ceramide induces serotonin release from RBL-2H3 mast cells through calcium mediated activation of phospholipase A2, Prostaglandins Other Lipid Mediat 94 (2011) 88-95.

[18] N.L. Cross, Sphingomyelin modulates capacitation of human sperm in vitro, Biol Reprod 63 (2000) 1129-1134.

[19] T. Murase, N. Imaeda, N. Kondoh, T. Tsubota, Ceramide enhances acrosomal exocytosis triggered by calcium and the calcium ionophore A23187 in boar spermatozoa, J Reprod Dev 50 (2004) 667-674.

[20] L. Suhaiman, G.A. De Blas, L.M. Obeid, A. Darszon, L.S. Mayorga, S.A. Belmonte, Sphingosine 1-phosphate and sphingosine kinase are involved in a novel signaling pathway leading to acrosomal exocytosis, J.Biol.Chem. 285 (2010) 16302-16314.

[21] C. Mendoza, A. Carreras, J. Moos, J. Tesarik, Distinction between true acrosome reaction and degenerative acrosome loss by a one-step staining method using Pisum sativum agglutinin, J.Reprod.Fertil. 95 (1992) 755-763.

[22] S.A. Belmonte, L. Suhaiman, Optimized protocols to analyze sphingosine-1-phosphate signal transduction pathways during acrosomal exocytosis in human sperm, Methods Mol.Biol. 874 (2012) 99-128.

[23] C.I. Lopez, S.A. Belmonte, G.A. De Blas, L.S. Mayorga, Membrane-permeant Rab3A triggers acrosomal exocytosis in living human sperm, FASEB J. 21 (2007) 4121-4130.

[24] O. Lucchesi, M.C. Ruete, M.A. Bustos, M.F. Quevedo, C.N. Tomes, The signaling module cAMP/Epac/Rap1/PLCepsilon/IP3 mobilizes acrosomal calcium during sperm exocytosis, Biochim Biophys Acta 1863 (2016) 544-561.

[25] V.E. Zarelli, M.C. Ruete, C.M. Roggero, L.S. Mayorga, C.N. Tomes, PTP1B dephosphorylates NSF and elicits SNARE complex disassembly during human sperm exocytosis, J.Biol.Chem. (2009).
[26] L.E. Pelletan, L. Suhaiman, C.C. Vaquer, M.A. Bustos, G.A. De Blas, N. Vitale, L.S. Mayorga, S.A. Belmonte, ADP Ribosylation Factor 6 (ARF6) Promotes Acrosomal Exocytosis by Modulating Lipid Turnover and Rab3A Activation, J.Biol.Chem. (2015).
[27] E.S. Reynolds, The use of lead citrate at high pH as an electron-opaque stain in electron microscopy, J Cell Biol 17 (1963) 208-212.
[28] A.D. Losinno, V. Sorrivas, M. Ezquer, F. Ezquer, L.A. Lopez, A. Morales, Changes of myoid and endothelial cells in the peritubular wall during contraction of the seminiferous tubule, Cell Tissue Res 365 (2016) 425-435.
[29] L. Mayorga, K. Altamirano, E. Zanni Ruiz, M. Pavarotti, Human sperm capacitation is necessary for SNARE assembly in neurotoxin-resistant complexes, Andrology (2019).
[30] E. Tada, K. Toyomura, H. Nakamura, H. Sasaki, T. Saito, M. Kaneko, Y. Okuma, T. Murayama, Activation of ceramidase and ceramide kinase by vanadate via a tyrosine kinase-mediated pathway, J.Pharmacol.Sci. 114 (2010) 420-432.
[31] C.A. Pocognoni, G.A. De Blas, A.P. Heuck, S.A. Belmonte, L.S. Mayorga, Perfringolysin O as a useful tool to study human sperm physiology, Fertil.Steril. 99 (2013) 99-106.
[32] I. Ramirez-Camacho, R. Bautista-Perez, F. Correa, M. Buelna-Chontal, N.G. Roman-Anguiano, M. Medel-Franco, O.N. Medina-Campos, J. Pedraza-Chaverri, A. Cano-Martinez, C. Zazueta, Role of sphingomyelinase in mitochondrial ceramide accumulation during reperfusion, Biochim Biophys Acta 1862 (2016) 1955-1963.
[33] F.M. Flesch, B.M. Gadella, Dynamics of the mammalian sperm plasma membrane in the process of fertilization, Biochim.Biophys.Acta 1469 (2000) 197-235.
[34] J.L. Dacheux, F. Dacheux, New insights into epididymal function in relation to sperm maturation, Reproduction 147 (2014) R27-42.
[35] A. Asano, J.L. Nelson-Harrington, A.J. Travis, Phospholipase B is activated in response to sterol removal and stimulates acrosome exocytosis in murine sperm, J Biol Chem 288 (2013) 28104-28115.
[36] P.E. Visconti, Understanding the molecular basis of sperm capacitation through kinase design, Proc.Natl.Acad.Sci.U.S.A 106 (2009) 667-668.
[37] S.A. Belmonte, L.S. Mayorga, C.N. Tomes, The Molecules of Sperm Exocytosis, Adv Anat Embryol Cell Biol 220 (2016) 71-92.
[38] C.R. Austin, The capacitation of the mammalian sperm, Nature 170 (1952) 326.
[39] M.C. Chang, Fertilizing capacity of spermatozoa deposited into the fallopian tubes, Nature 168 (1951) 697-698.
[40] M. Muratori, M. Luconi, S. Marchiani, G. Forti, E. Baldi, Molecular markers of human sperm functions, Int.J.Androl (2008).
[41] S.A. Belmonte, C.I. Lopez, C.M. Roggero, G.A. De Blas, C.N. Tomes, L.S. Mayorga, Cholesterol content regulates acrosomal exocytosis by enhancing Rab3A plasma membrane association, Dev.Biol. 285 (2005) 393-408.
[42] K.J. French, R.S. Schrecengost, B.D. Lee, Y. Zhuang, S.N. Smith, J.L. Eberly, J.K. Yun, C.D. Smith, Discovery and evaluation of inhibitors of human sphingosine kinase, Cancer Res. 63 (2003) 5962-5969.
[43] N. Zanetti, L.S. Mayorga, Acrosomal swelling and membrane docking are required for hybrid vesicle formation during the human sperm acrosome reaction, Biol.Reprod. 81 (2009) 396-405.

[44] C.M. Sosa, M.N. Zanetti, C.A. Pocognoni, L.S. Mayorga, Acrosomal Swelling Is Triggered by cAMP Downstream of the Opening of Store-Operated Calcium Channels During Acrosomal Exocytosis in Human Sperm, Biol Reprod 94 (2016) 57.

[45] G.A. De Blas, C.M. Roggero, C.N. Tomes, L.S. Mayorga, Dynamics of SNARE assembly and disassembly during sperm acrosomal exocytosis, PLoS.Biol., 2005.

[46] W. Sun, R. Xu, W. Hu, J. Jin, H.A. Crellin, J. Bielawski, Z.M. Szulc, B.H. Thiers, L.M. Obeid, C. Mao, Upregulation of the human alkaline ceramidase 1 and acid ceramidase mediates calcium-induced differentiation of epidermal keratinocytes, J Invest Dermatol 128 (2008) 389-397.

[47] N.E. Furland, G.M. Oresti, S.S. Antollini, A. Venturino, E.N. Maldonado, M.I. Aveldano, Very long-chain polyunsaturated fatty acids are the major acyl groups of sphingomyelins and ceramides in the head of mammalian spermatozoa, J.Biol.Chem. 282 (2007) 18151-18161.

[48] G.M. Oresti, J.G. Reyes, J.M. Luquez, N. Osses, N.E. Furland, M.I. Aveldano, Differentiation-related changes in lipid classes with long-chain and very long-chain polyenoic fatty acids in rat spermatogenic cells, J Lipid Res 51 (2010) 2909-2921.

[49] G.M. Oresti, D.A. Penalva, J.M. Luquez, S.S. Antollini, M.I. Aveldano, Lipid Biochemical and Biophysical Changes in Rat Spermatozoa During Isolation and Functional Activation In Vitro, Biol Reprod 93 (2015) 140.

[50] S.R. Zanetti, M.M. de Los Angeles, D.E. Rensetti, M.W. Fornes, M.I. Aveldano, Ceramides with 2-hydroxylated, very long-chain polyenoic fatty acids in rodents: From testis to fertilization-competent spermatozoa, Biochimie 92 (2010) 1778-1786.

[51] M. Raisova, G. Goltz, M. Bektas, A. Bielawska, C. Riebeling, A.M. Hossini, J. Eberle, Y.A. Hannun, C.E. Orfanos, C.C. Geilen, Bcl-2 overexpression prevents apoptosis induced by ceramidase inhibitors in malignant melanoma and HaCaT keratinocytes, FEBS Lett 516 (2002) 47-52.

[52] A. Lepple-Wienhues, C. Belka, T. Laun, A. Jekle, B. Walter, U. Wieland, M. Welz, L. Heil, J. Kun, G. Busch, M. Weller, M. Bamberg, E. Gulbins, F. Lang, Stimulation of CD95 (Fas) blocks T lymphocyte calcium channels through sphingomyelinase and sphingolipids, Proc Natl Acad Sci U S A 96 (1999) 13795-13800.

[53] D.P. Relling, K.K. Hintz, J. Ren, Acute exposure of ceramide enhances cardiac contractile function in isolated ventricular myocytes, Br J Pharmacol 140 (2003) 1163-1168.

[54] C. Beltran, C.L. Trevino, E. Mata-Martinez, J.C. Chavez, C. Sanchez-Cardenas, M. Baker, A. Darszon, Role of Ion Channels in the Sperm Acrosome Reaction, Adv Anat Embryol Cell Biol 220 (2016) 35-69.

[55] J.C. Kirkman-Brown, C.L. Barratt, S.J. Publicover, Nifedipine reveals the existence of two discrete components of the progesterone-induced [Ca2+]i transient in human spermatozoa, Dev.Biol. 259 (2003) 71-82.

[56] A. Darszon, T. Nishigaki, C. Beltran, C.L. Trevino, Calcium channels in the development, maturation, and function of spermatozoa, Physiol Rev. 91 (2011) 1305-1355.

[57] M.K. Jungnickel, H. Marrero, L. Birnbaumer, J.R. Lemos, H.M. Florman, Trp2 regulates entry of Ca2+ into mouse sperm triggered by egg ZP3, Nat.Cell Biol. 3 (2001) 499-502.

[58] C.V. Harper, C.L. Barratt, S.J. Publicover, Stimulation of human spermatozoa with progesterone gradients to simulate approach to the oocyte. Induction of [Ca(2+)](i) oscillations and cyclical transitions in flagellar beating, J Biol Chem 279 (2004) 46315-46325.

[59] C.V. Harper, S.J. Publicover, Reassessing the role of progesterone in fertilization--compartmentalized calcium signalling in human spermatozoa?, Hum Reprod 20 (2005) 2675-2680.

[60] S.S. Suarez, Control of hyperactivation in sperm, Hum Reprod Update 14 (2008) 647-657.

[61] Y. Zhou, Y. Ru, C. Wang, S. Wang, Z. Zhou, Y. Zhang, Tripeptidyl peptidase II regulates sperm function by modulating intracellular Ca(2+) stores via the ryanodine receptor, PLoS One 8 (2013) e66634.

[62] T. Yoshino, J. Ishikawa, K. Ohga, T. Morokata, R. Takezawa, H. Morio, Y. Okada, K. Honda, T. Yamada, YM-58483, a selective CRAC channel inhibitor, prevents antigen-induced airway eosinophilia and late phase asthmatic responses via Th2 cytokine inhibition in animal models, Eur.J.Pharmacol. 560 (2007) 225-233.

[63] B.A. Kachoei, R.J. Knox, D. Uthuza, S. Levy, L.K. Kaczmarek, N.S. Magoski, A store-operated Ca(2+) influx pathway in the bag cell neurons of Aplysia, J.Neurophysiol. 96 (2006) 2688-2698.

[64] C.L. Trevino, D.l.V.-B. JL, T. Nishigaki, R. Felix, A. Darszon, Maitotoxin potently promotes Ca2+ influx in mouse spermatogenic cells and sperm, and induces the acrosome reaction, J.Cell Physiol 206 (2006) 449-456.

[65] N. Mannowetz, M.R. Miller, P.V. Lishko, Regulation of the sperm calcium channel CatSper by endogenous steroids and plant triterpenoids, Proc Natl Acad Sci U S A 114 (2017) 5743-5748.

[66] P.V. Lishko, I.L. Botchkina, Y. Kirichok, Progesterone activates the principal Ca2+ channel of human sperm, Nature 471 (2011) 387-391.

[67] A. Darszon, C. Sanchez-Cardenas, G. Orta, A.A. Sanchez-Tusie, C. Beltran, I. Lopez-Gonzalez, G. Granados-Gonzalez, C.L. Trevino, Are TRP channels involved in sperm development and function?, Cell Tissue Res 349 (2012) 749-764.

[68] C.I. Lopez, L.E. Pelletan, L. Suhaiman, G.A. De Blas, N. Vitale, L.S. Mayorga, S.A. Belmonte, Diacylglycerol stimulates acrosomal exocytosis by feeding into a PKC- and PLD1-dependent positive loop that continuously supplies phosphatidylinositol 4,5-bisphosphate, Biochim.Biophys.Acta 1821 (2012) 1186-1199.

[69] V.T. Hinkovska, D.H. Petkova, K.S. Koumanov, A neutral sphingomyelinase in spermatozoal plasma membranes, Biochem Cell Biol 65 (1987) 525-528.

[70] G. Wang, Y. Guo, T. Zhou, X. Shi, J. Yu, Y. Yang, Y. Wu, J. Wang, M. Liu, X. Chen, W. Tu, Y. Zeng, M. Jiang, S. Li, P. Zhang, Q. Zhou, B. Zheng, C. Yu, Z. Zhou, X. Guo, J. Sha, In-depth proteomic analysis of the human sperm reveals complex protein compositions, J.Proteomics. 79 (2013) 114-122.

[71] M.R. Miller, N. Mannowetz, A.T. Iavarone, R. Safavi, E.O. Gracheva, J.F. Smith, R.Z. Hill, D.M. Bautista, Y. Kirichok, P.V. Lishko, Unconventional endocannabinoid signaling governs sperm activation via the sex hormone progesterone, Science 352 (2016) 555-559.

[72] J.M. Holopainen, M.I. Angelova, P.K. Kinnunen, Vectorial budding of vesicles by asymmetrical enzymatic formation of ceramide in giant liposomes, Biophys J 78 (2000) 830-838.

[73] S. Costello, F. Michelangeli, K. Nash, L. Lefievre, J. Morris, G. hado-Oliveira, C. Barratt, J. Kirkman-Brown, S. Publicover, Ca2+-stores in sperm: their identities and functions, Reproduction. 138 (2009) 425-437.

[74] P.V. Lishko, Y. Kirichok, D. Ren, B. Navarro, J.J. Chung, D.E. Clapham, The control of male fertility by spermatozoan ion channels, Annu Rev Physiol 74 (2012) 453-475.

[75] K. Fukami, M. Yoshida, T. Inoue, M. Kurokawa, R.A. Fissore, N. Yoshida, K. Mikoshiba, T. Takenawa, Phospholipase Cdelta4 is required for Ca2+ mobilization essential for acrosome reaction in sperm, J Cell Biol 161 (2003) 79-88.

[76] J. Xia, D. Ren, Egg coat proteins activate calcium entry into mouse sperm via CATSPER channels, Biol Reprod 80 (2009) 1092-1098.

[77] N. Leblanc, J.R. Hume, Sodium current-induced release of calcium from cardiac sarcoplasmic reticulum, Science 248 (1990) 372-376.

[78] S. Pitake, R.S. Ochs, Membrane depolarization increases ryanodine sensitivity to Ca2+ release to the cytosol in L6 skeletal muscle cells: Implications for excitation-contraction coupling, Exp Biol Med (Maywood) 241 (2016) 854-862.

[79] C.L. Chik, B. Li, E. Karpinski, A.K. Ho, Ceramide inhibits L-type calcium channel currents in GH3 cells, Mol.Cell Endocrinol. 218 (2004) 175-183.
[80] C.L. Chik, B. Li, E. Karpinski, A.K. Ho, Ceramide inhibits the outward potassium current in rat pinealocytes, J.Neurochem. 79 (2001) 339-348.
[81] J. Bock, I. Szabo, N. Gamper, C. Adams, E. Gulbins, Ceramide inhibits the potassium channel Kv1.3 by the formation of membrane platforms, Biochem Biophys Res Commun 305 (2003) 890-897.
[82] C. Stival, F.A. La Spina, C. Baro Graf, E. Arcelay, S.E. Arranz, J.J. Ferreira, S. Le Grand, V.A. Dzikunu, C.M. Santi, P.E. Visconti, M.G. Buffone, D. Krapf, Src Kinase Is the Connecting Player between Protein Kinase A (PKA) Activation and Hyperpolarization through SLO3 Potassium Channel Regulation in Mouse Sperm, J Biol Chem 290 (2015) 18855-18864.
[83] W. Jin, A. Tanaka, G. Watanabe, H. Matsuda, K. Taya, Effect of NGF on the motility and acrosome reaction of golden hamster spermatozoa in vitro, J.Reprod.Dev. 56 (2010) 437-443.
[84] K. Lin, X.F. Ding, C.G. Shi, D. Zeng, S. QuZong, S.H. Liu, Y. Wu, G. LuoBu, M. Fan, Y.Q. Zhao, Nerve growth factor promotes human sperm motility in vitro by increasing the movement distance and the number of A grade spermatozoa, Andrologia 47 (2015) 1041-1046.
[85] Y. Kirichok, B. Navarro, D.E. Clapham, Whole-cell patch-clamp measurements of spermatozoa reveal an alkaline-activated Ca2+ channel, Nature 439 (2006) 737-740.
[86] T. Strunker, N. Goodwin, C. Brenker, N.D. Kashikar, I. Weyand, R. Seifert, U.B. Kaupp, The CatSper channel mediates progesterone-induced Ca2+ influx in human sperm, Nature 471 (2011) 382-386.
[87] N. Marchesini, W. Osta, J. Bielawski, C. Luberto, L.M. Obeid, Y.A. Hannun, Role for mammalian neutral sphingomyelinase 2 in confluence-induced growth arrest of MCF7 cells, J.Biol.Chem. 279 (2004) 25101-25111.
[88] J.P. Jaffrezou, N. Maestre, V. de Mas-Mansat, C. Bezombes, T. Levade, G. Laurent, Positive feedback control of neutral sphingomyelinase activity by ceramide, FASEB J 12 (1998) 999-1006.
[89] G. De Blas, M. Michaut, C.L. Trevino, C.N. Tomes, R. Yunes, A. Darszon, L.S. Mayorga, The intraacrosomal calcium pool plays a direct role in acrosomal exocytosis, J.Biol.Chem. 277 (2002) 49326-49331.

Legend to figures

Figure 1. Enzymes involved in sphingolipid metabolism are present in human spermatozoa. (A, C) Whole sperm proteins (25×10^6 sperm/ml) were extracted according to Methods and analyzed by Western blot with antibodies directed against the indicated enzymes. (A) neutral sphingomyelinase 2 (nSMase2, 48 kDa); (C) Ceramide synthase (CerS, 46 kDa). As positive control for WB HeLa extracts (A,

C) were used. Molecular mass standards (kDa) are indicated on the right. (B) and (D). Localization of the enzymes was analyzed by indirect inmunofluorescence using the same antibodies that were used for WB experiments according to Methods. The cells were fixed and double-stained with anti-nSMase2 (B) or anti-CerS (D) antibodies, followed by an anti-rabbit Cy3 (red) and FITC-PSA to differentiate between reacted and intact sperm (green). The merged images are shown. Inmunofluorescence images were obtained using a Confocal Olympus FluoViewTM FV1000 software FV10-ASW (version 01.07.00.16).

Figure 2. C6-ceramide triggers acrosomal exocytosis in capacitated human spermatozoa in a sphingosine 1-phosphate independent manner. (A) Capacitated sperm were treated with increasing concentrations of C6-ceramide (C6-Cer, C6, 0.5–25 μM) for 15 min at 37°C. As positive control, sperm were treated with 15 μM Pg. Sperm were fixed and acrosomal exocytosis was evaluated by FITC-PSA binding with at least 300 cells per condition scored. The data represent the mean ± S.E. from three to five independent experiments. Tukey-Kramer´s test was used to compare the means of groups against the Pg stimulated condition and classified as significant: (***, $p < 0.001$; **, $p < 0.01$) or non-significant (ns, $p > 0.05$). (B) An aliquot of a sperm sample was subjected to swim-up in HTF medium under non-capacitating (non-cap) conditions (37°C, 5% CO_2, without bovine serum albumin) and treated right away as described below. Another aliquot was processed in capacitating conditions (cap): swim-up in HTF (5 mg/ml bovine serum albumin, 37°C, 5% CO_2) and incubated for an additional 2 h. Capacitated and non-capacitated sperm were treated or

not (control, Co) with 15 μM Pg or 10 μM C6-Cer for 15 min at 37°C, 5% CO_2. Acrosomal exocytosis was evaluated as explained under "*Materials & methods*". The data represent the mean ± S.E. of at least four independent experiments. The means of groups were compared with Pg under capacitating conditions using Dunnett's test and classified as non-significant (ns, $p > 0.05$) or significant (***, $p < 0.001$). (C) Capacitated spermatozoa were incubated at 37°C for 15 min without any stimulus (control, Co) or treated with 15 μM Pg or 10 μM C6-Cer. When indicated cells treated with C6-Cer (C6) were further incubated with Pg for 15 additional min (C6→Pg). The data represent the mean ± S.E. of at least three independent experiments. Tukey-Kramer test was used to compare the means of groups against the Pg stimulated condition and classified as significant (*, $p < 0.05$) or non-significant (ns, $p > 0.05$). (D) Capacitated spermatozoa were incubated at 37°C for 15 min without any stimulus (control, Co) or treated with 10 μM diacylglycerol (DAG) or 10 μM C6-Cer (C6) at 37°C for 15 min. When indicated cells treated with C6-Cer were further incubated with DAG for 15 additional min (C6→DAG). The data represent the mean ± S.E. of at least three independent experiments. Tukey-Kramer´s test was used to compare the means of groups against the DAG stimulated condition and classified as non-significant (ns, $p > 0.05$). (E) Scheme depicting part of the signaling pathway of sphingolipids (CDase: ceramidase, SK: sphingosine kinase, S1P: sphingosine 1-phosphate). Ceramide can be broken down by one of many ceramidases, leading to the formation of sphingosine, which can be phosphorylated by SK to synthesize S1P. (F) Capacitated sperm were treated with 1 μM SKI

(sphingosine kinase inhibitor) and were further incubated for 15 min in the absence of any stimulus (Co), in the presence of 200 nM PMA or 10 μM C6-Cer. The data represent the mean ± S.E. of at least five independent experiments. s, *** $P < 0.001$; ns, $P > 0.05$ (Tukey-Kramer´s test).

Figure 3. C6-Cer addition induces physiological ultrastructural changes in the acrosome and a signaling cascade involving PTP1B and VAMP2. (A) Cells were incubated for 2 h under capacitating conditions and treated for 15 min at 37°C in the presence of 10 μM C6-Cer or 10 μM A23187 and processed as described in "*Materials & methods*" for electron microscopy. Transmission electron micrographs of spermatozoa after C6-Cer treatment showing different morphological stages: intact, swollen+waving with vesicles and reacted. pm: plasma membrane; oam: outer acrosomal membrane; iam: inner acrosomal membrane; nm nuclear membrane; es: equatorial segment; v: vesicle; †: swollen acrosome. Scale bars, 500 nm and 3 μm. (B) Quantification of the percentage of intact, swollen (swollen and waving with vesicles) and reacted sperm (lost acrosomes). The means of groups swollen plus waving with vesicles were compared with the corresponding control s, * $P < 0.05$; ns, $P > 0.05$ (Newman-Keuls Multiple Comparison Test). (C) Scheme depicting the role of PTP1B in the signaling cascade leading to membrane fusion (NSF: N-ethylmaleimide-sensitive factor, P: phosphorylated; SNARE: SNAP receptor). Rab 3A activation direct or indirectly induces NSF dephosphorylation. Then, active NSF drives cis-SNARE complex disassembly rendering fusion competent SNAREs. (D) Capacitated human sperm were incubated with or without 0.25 mM

photosensitive-PTP inhibitor I (PTPi) for 10 min at 37°C in the dark. When indicated 15 μM Pg (Pg, PTPi→Pg) or 10 μM C6 (C6, PTPi→C6) were added in the dark. After 10 min incubation the tubes were illuminated with U.V. light to reverse the block on PTP (PTPi→h.ν, PTPi→Pg→h.ν; PTPi→C6→h.ν) two times 1 min each, and further incubated 5 min at 37°C. Sperm were fixed and acrosome reaction was measured by FITC-PSA binding as described in "*Materials & Methods*". Several controls were run: inhibitory effect of PTP Inhibitor I in the dark (PTPi, PTPi→Pg, PTPi→C6) and upon illumination, (PTPi→h.ν). As a positive control Pg was used. The data represent the mean ± S.E. of at least three independent experiments. Dunnett´s test was used to compare the means of groups against the Pg or C6 stimulated condition and classified as significant (***, $p < 0.001$) or non-significant (ns, $p > 0.05$). E: Capacitated sperm were treated with 1.5 μM recombinant cell-permeant Tetanus toxin (Te-Tx) for 15 min at 37°C in 5% CO_2. When indicated cells were challenged with 10 μM A23187 (A23187, Te-Tx→A23187) or 10 μM C6-Cer (C6, Te-Tx→C6) for an additional 15 min. The data represent the mean ± S.E. of at least four independent experiments. Dunnett´s test was used to compare the means of groups against the corresponding control: A23187 and C6-Cer stimulated conditions and classified as significant (*** $p < 0.001$; ** $p \leq 0.01$).

(E) Sperm were treated with 1.5 μM recombinant cell-permeant Tetanus toxin (Te-Tx) for 15 min at 37°C. When indicated cells were challenged with 10 μM A23187 or 10 μM C6-Cer (15 min). Data represent the mean ± S.E. of at least four independent experiments. Dunnett´s test was used to compare the means of groups against the control and stimulated conditions. Significant (*** $P < 0.001$; ** $P \leq 0.01$).

Figure 4. Ceramidases are present and active in human sperm and endogenous ceramide increase induces acrosomal exocytosis. (A) Whole sperm proteins (25×10^6 sperm/ml) were extracted as described in Methods and analyzed by Western blot with an antibody directed against neutral ceramidase (nCDase, 84 kDa). As positive control for WB mouse testis extract was used. Molecular mass standards (kDa) are indicated on the right. (B) Localization of the enzymes was analyzed by indirect inmunofluorescence using the same antibody used for WB experiment according to Methods. The cells were fixed and double-stained with anti-nCDase antibody, followed by an anti-rabbit Cy3 (red) and FITC-PSA to differentiate between reacted and intact sperm (green). The merged images are shown. (C) Capacitated human spermatozoa were loaded with cell-permeant C12-NBD (10 μM) during 1 h. Afterwards, cells were treated or not with 10 μM D-NMAPPD 15 min, and when indicated cells were challenged with 10 μM A23187. Samples were further incubated for 15 min at 37°C. Lipid extraction was performed as

described according to Tada et al (2010) [30]. Thin-layer chromatograms were developed in 1-butanol/acetic acid/water (3:1:1 v/v) as solvent system and visualized by fluorescence intensity. (D) Quantification of spot intensity of thin-layer chromatogram of figure (C) corresponding to lauric acid. (E) After swim-up in HTF (5 mg/ml BSA) at 37°C, 5% CO_2, sperm were incubated for an additional 2 h under capacitating conditions. Then, they were treated with increasing concentrations of D-NMAPPD (10–50 μM) for 15 min at 37°C in 5% CO_2. As positive control, sperm were treated with 15 μM Pg. Sperm were fixed and acrosomal exocytosis was evaluated by FITC-PSA binding with at least 300 cells per condition scored. One way ANOVA and Dunnett´s test were used to compare the means against the corresponding Pg-stimulated condition and classified as non-significant (ns, $p > 0.05$).

Figure 5. Ceramide increase induces an $[Ca^{2+}]i$ rise in live human sperm. (A) Capacitated human sperm recovered after swim-up were loaded with Fluo-3AM (2 μM) and the fluorescence intensity was visualized before and after C6-Cer addition as described under Methods. Representative single cell spatiotemporal $[Ca^{2+}]i$ changes (0 and 6.25 sec) before and after adding 10 μM C6-Cer (12.5, 18.75, 25). Ionomycin (20 μM) was added at the end of the experiment as positive control (not shown). The time frame is indicated in each panel (seconds). The color bar shows fluorescence intensity after background subtraction. (B) Summarizes the C6-Cer response (red bar) compared to Ionomycin (yellow bar). Δ(F/F0)-1 is the average of the changes in fluorescence of all individual human sperm analyzed (C6, N=3, 135

cells) and Ionomycin (N=3, 67 cells). Error bars represent the mean ± S.E. Dunnett's test was used to compare the means of C6-Cer against the Ionomycin condition and classified as non-significant (ns, P > 0.05). (C-E)**.** Human sperm were loaded with 2 μM Fluo 3-AM and incubated for 30 min at 37°C. At the indicated times (*arrows*) 15 μM Pg (C), 10 μM C6-Cer (D), or 10 μM D-NMAPPD (E) were added. Maximal $[Ca^{2+}]$i response was calibrated by adding 0.1% Triton X-100 (TX-100) at the end of the incubation period. Shown are traces representative of five experiments. The increase in fluorescence is expressed as (*F*/*F*0)-1 ((maximum fluorescence intensity/initial fluorescence)-1) *versus* time in seconds. (F**)** Δ(F/F0)-1 is the average of the changes in fluorescence of batches analyzed. Bars represent mean ± S.E. of five experiments, data were normalized against the calcium response to Pg. Dunnett´s test was used to compare the means of groups against calcium response induced by Pg (positive control) and classified as non-significant (ns, P > 0.05).

Figure 6. Ceramide increase promotes calcium mobilization from internal stores but it is not enough to induce exocytosis. (A-C) Sperm were loaded with 2 μM Fluo-3AM for 30 min at 37°C, washed and, suspended in a media containing 0.75 mM EGTA, 0.5 mM Ca^{2+} (≤100 nM free calcium estimated by MAXCHELATOR). At the indicated times (*arrows*) (A) 15 μM Pg, (B) 10 μM C6-Cer or (C) 10 μM D-NMAPPD were added. Maximal $[Ca^{2+}]$i response was calibrated with 0.1% Triton X-100 at the end of the incubation period. Shown are traces representative of five experiments. The increase in fluorescence is expressed as (F/F0)-1 (maximum fluorescence intensity/initial fluorescence)-1) versus time in seconds. (D) Bars represent mean ± S.E.

of six experiments (data from figures 6 (C, D, and E) and 7 (A, B, and C); data were normalized against the calcium response to 15 μM Pg. The means were compared to the positive control (Pg, in a calcium containing media) using Dunnett test and classified as non-significant (ns, P> 0.05); or significant: (*, P< 0.05 or **, P ≤ 0.01 or, ***P ≤ 0.001). (E) Spermatozoa were kept in a 2 mM Ca^{2+} media (solid bars) or in a [Ca^{2+}] ≤ 100nM media (white bars). Samples were incubated for a further 15 min in the absence of any stimulus (Co), with 15 μM Pg, 10 μM C6-Cer, or 10 μM D-NMPAAD. Each condition was compared to Pg treatment (2 mM Ca^{2+}) using Dunnett´s test and classified as non-significant (ns > 0.05) or significant (* P ≤ 0.05; ** P ≤ 0.01). (F) Sperm were incubated for 15 min without any stimulus (Co) or when indicated with 5 mM BAPTA 15 min at 37 °C. Samples were incubated for a further 15 min with 10μM C6-Cer. The data represent the mean ± S.E. from three to five independent experiments. The means of groups were compared with the C6-Cer conditions using Dunnett´s test. Significant (*** P ≤ 0.001).

Figure 7. C6-Cer-induced calcium mobilization involves the activation of ryanodine receptors, CatSper, and SOCCs. Capacitated human sperm recovered after swim-up were loaded with Fluo-3AM (2 μM), and the fluorescence intensity was visualized as described under Methods. Representative spatiotemporal [Ca^{2+}]i changes and their corresponding traces are shown. The arrow indicates the addition of 10 μM C6-Cer, and the red trace has no other addition. When indicated cells were preincubated for 15 min at 37°C with: (A**)** 100 mM Verapamil, (B) 100 mM 2-APB, (C) 100 mM Xestospongin C (XC),

(D) 20 nM ruthenium red (RR), (E) 1 μM YM-58483 (YM), (F) 50 μM SKF-96365 (SKF), (G) 1 μM NNC 55–0396 (NNC). (H) ΔF(F/F0)-1) is the average of the changes in fluorescence of each condition measured. Bars represent mean ± S.E. Different conditions were compared using Dunnett´s test and C6-Cer as a control, and differences were classified as non-significant (ns, $P > 0.05$) or significant (** $P \leq 0.01$; *** $P \leq 0.001$). **I.** Capacitated sperm were incubated without any treatment (control, Co) or treated when indicated with 100 mM Verapamil, 100 mM 2-APB, 100 mM XC, 20 nM RR, 1 μM YM, 50 μM SKF, or 1 μM NNC for 15 min at 37°C. When specified, acrosomal exocytosis was initiated by adding 10 μM C6-Cer and the incubation continued for an additional 15 min. Sperm were then fixed, and acrosomal exocytosis was measured. The data represent the mean ± S.E. from 3 to 14 independent experiments. Dunnett's test was used to compare the means of all groups against the C6-Cer-stimulated condition in the absence of inhibitors and classified as non-significant (ns, $P > 0.05$) or significant (*** $P \leq 0.001$).

Figure 8. Working model proposed for ceramide´s role in acrosomal exocytosis. In this model, we propose that progesterone and ceramide activates CatSper acting in concert under physiological conditions. The interaction of progesterone with its receptor generates arachidonic acid (AA) [71], which is known to activate a sphingomyelinase localized at the plasma membrane promoting ceramide synthesis [87]. Endogenous ceramide exerts various effects, for example, it activates CatSper and ryanodin sensitive-calcium channels (RyR) located in the redundant nuclear envelope (RNE), as

well as Store Operated Calcium Channels (SOCC) all of them contributing to the calcium mobilization towards the sperm head. Cytosolic calcium increase would activate PLC that hydrolyzes phosphatidylinositol 4,5-bisphosphate (PIP_2) to generate DAG and IP_3. IP_3 binds to IP_3-sensitive calcium channels on the stores leading to calcium efflux. The emptying of the stores stimulates the sustained opening of SOCCs at the plasma membrane. On the other hand, ceramide activates a signal transduction cascade involving the activity of protein tyrosine phosphatase 1B (PTP1B) which dephosphorylates NSF (N-ethylmaleimide-sensitive factor) and elicits SNARE (SNAP receptor) complex disassembly during human sperm exocytosis. So, the signaling cascade triggered by ceramide, as well as other inducers, branches in at least two arms that come back together at the end of the cascade. Both a local increase in calcium coming from IP_3-sensitive channels and SNAREs converge to accomplish the final steps of membrane fusion. SK/S1P pathway seems to follow a pathway independent of acute ceramide increase. Our results suggest that ceramide could be involved in early stages of the exocytosis and after that, when calcium increase steadily, activities of ceramidase hydrolyzes ceramide leading to the generation of new second messengers.

Credit Author Statement

CCV carried out the majority of the AR assays, enzyme activity assays, electron microscopy experiments, calcium measurements, analyzed the data, and performed the statistical analysis. LS performed functional assays, composed the Figures, and participated in the writing, review, and editing. MAP developed the recombinant Te-Tx conjugated with a cell-penetrating peptide, carried out functional assays and analyzed the data. GADB carried out the calcium imaging studies and analyzed the data. SAB conceived of the research, designed, coordinated the work, funding acquisition, and wrote the manuscript. All authors read and approved the final manuscript.

Declaration

The work described has not been published previously; it is not under consideration for publication elsewhere, its publication is approved by all authors (consent included in the manuscript text) and tacitly by the responsible authorities of the IHEM, where the work was carried out. If accepted, it will not be published elsewhere in the same form, in English or in any other language, including electronically without the written consent of the copyright holder.

Highlights

- Ceramide induces intracellular calcium rise and acrosome secretion in human sperm
- The lipid activates RyR and calcium influx through CatSper (calcium channel of sperm) and SOCCs
- Ceramide induces acrosome physiological ultrastructural changes
- It triggers a signaling cascade involving protein tyrosine phosphatase 1B and VAMP2
- Ceramide concentration in membranes regulates exocytosis and fertilization

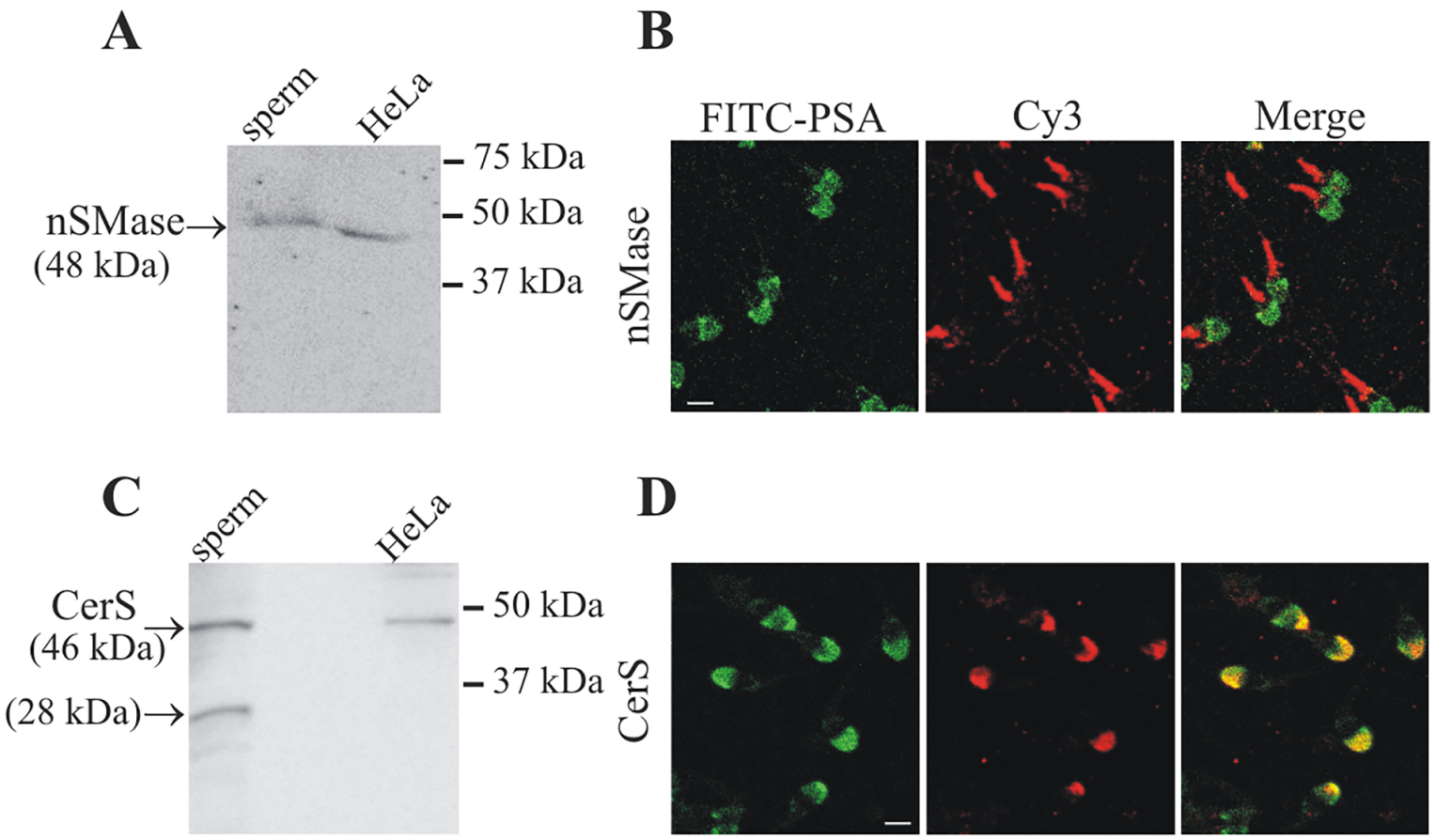
A
sperm
HeLa
nSMase→
(48 kDa)
75 kDa
50 kDa
37 kDa
B
FITC-PSA
Cy3
Merge
nSMase
C
sperm
HeLa
CerS
(46 kDa)→
(28 kDa)→
50 kDa
37 kDa
D
CerS

Figure 1

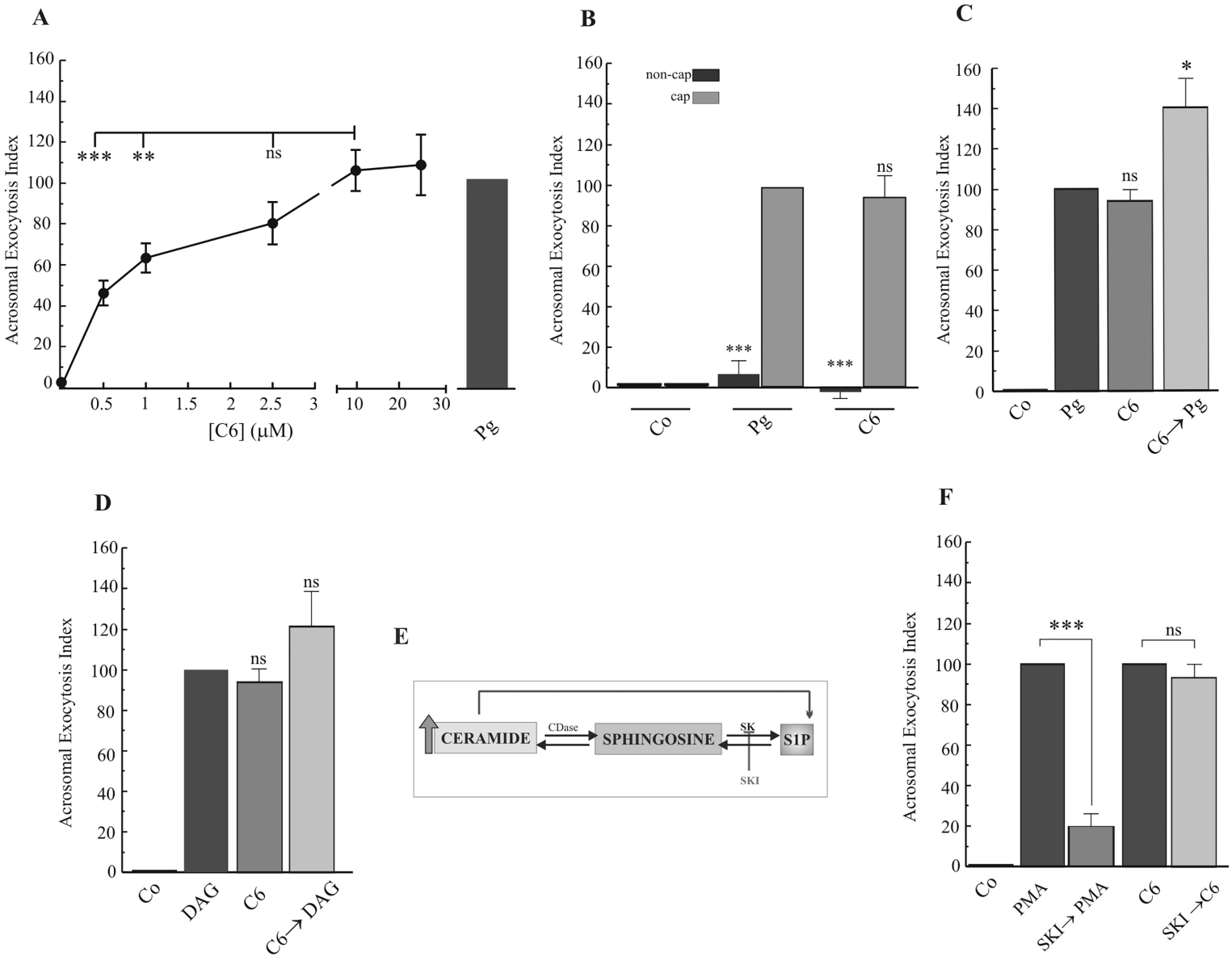
A
Acrosomal Exocytosis Index
[C6] (μM)
Pg
***
**
ns
B
non-cap
cap
Co
Pg
C6
C
Co
Pg
C6
C6→Pg
*
D
Co
DAG
C6
C6→DAG
E
CERAMIDE
CDase
SPHINGOSINE
SK
S1P
SKI
F
Co
PMA
SKI→PMA
C6
SKI→C6

Figure 2

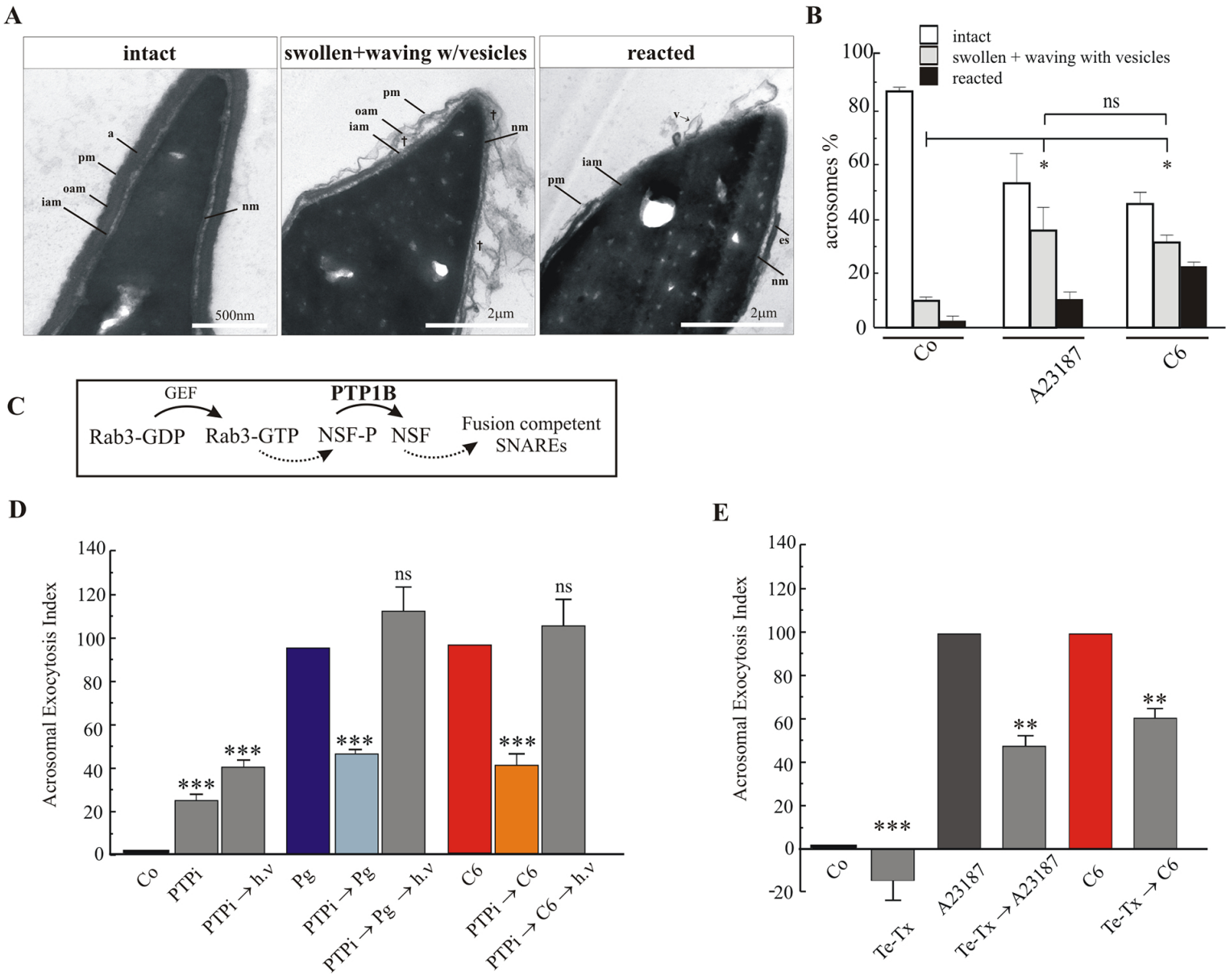
A
intact
swollen+waving w/vesicles
reacted
a
pm
oam
iam
nm
500nm
2µm
es
v
B
intact
swollen + waving with vesicles
reacted
acrosomes %
ns
*
Co
A23187
C6
C
GEF
PTP1B
Rab3-GDP
Rab3-GTP
NSF-P
NSF
Fusion competent SNAREs
D
Acrosomal Exocytosis Index
***
ns
Co
PTPi
PTPi → h.v
Pg
PTPi → Pg
PTPi → Pg → h.v
C6
PTPi → C6
PTPi → C6 → h.v
E
Acrosomal Exocytosis Index
**
Co
Te-Tx
A23187
Te-Tx → A23187
C6
Te-Tx → C6

Figure 3

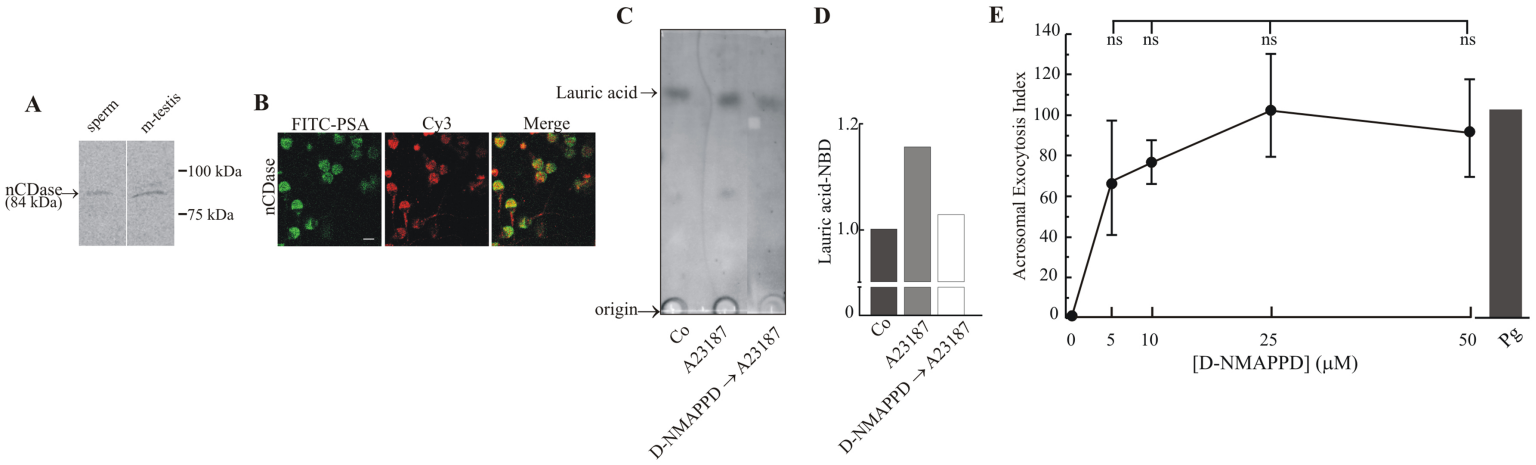
A
sperm
m-testis
nCDase
(84 kDa)
100 kDa
75 kDa
B
FITC-PSA
Cy3
Merge
nCDase
C
Lauric acid
origin
Co
A23187
D-NMAPPD → A23187
D
Lauric acid-NBD
1.2
1.0
0
Co
A23187
D-NMAPPD → A23187
E
ns
ns
ns
ns
Acrosomal Exocytosis Index
140
120
100
80
60
40
20
0
0
5
10
25
50
Pg
[D-NMAPPD] (μM)

Figure 4

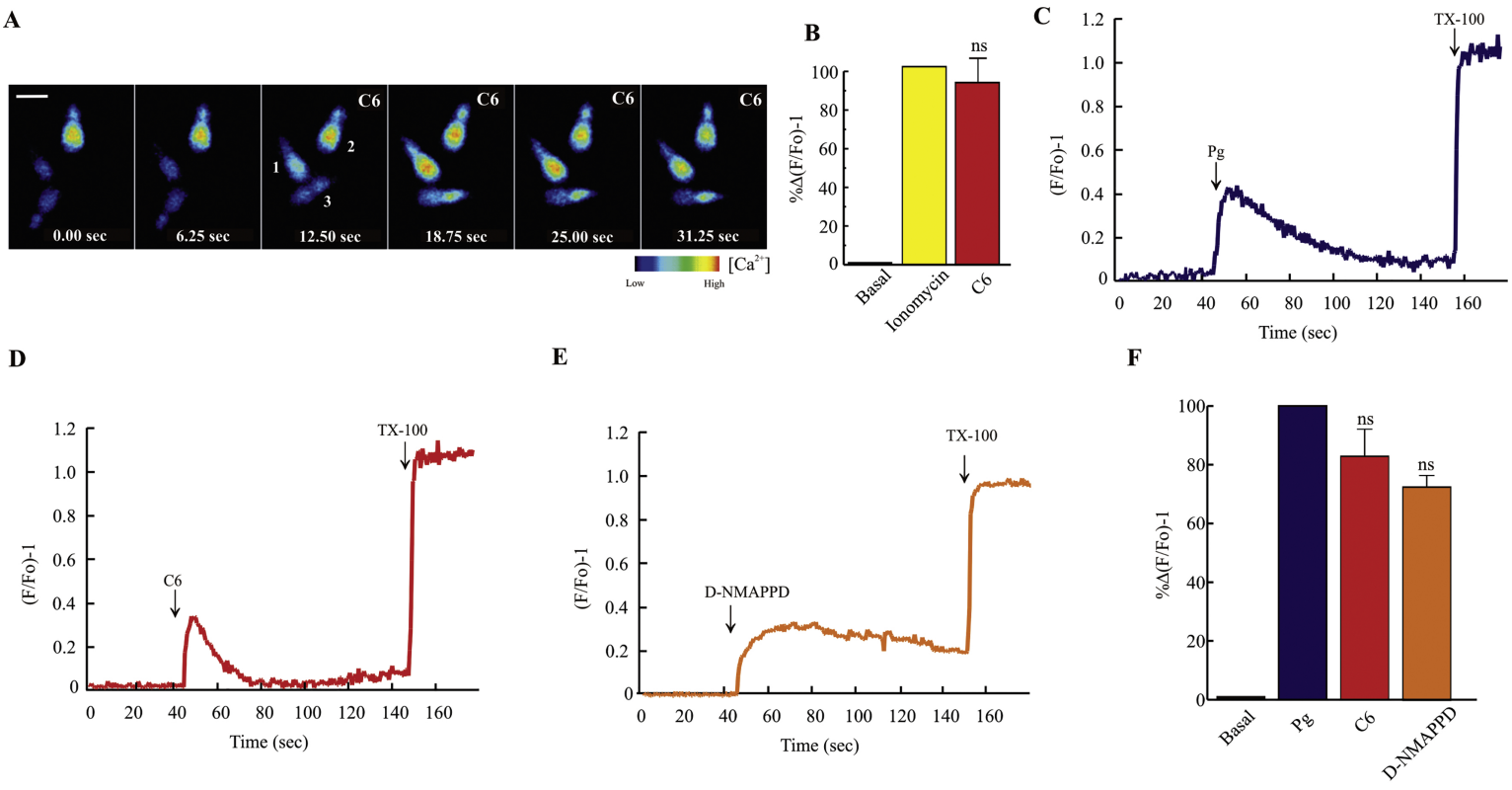
A
C6
1
2
3
0.00 sec
6.25 sec
12.50 sec
18.75 sec
25.00 sec
31.25 sec
[Ca2+]
Low
High
B
ns
%Δ(F/Fo)-1
Basal
Ionomycin
C6
C
TX-100
Pg
(F/Fo)-1
Time (sec)
D
C6
TX-100
(F/Fo)-1
Time (sec)
E
D-NMAPPD
TX-100
(F/Fo)-1
Time (sec)
F
ns
ns
%Δ(F/Fo)-1
Basal
Pg
C6
D-NMAPPD

Figure 5

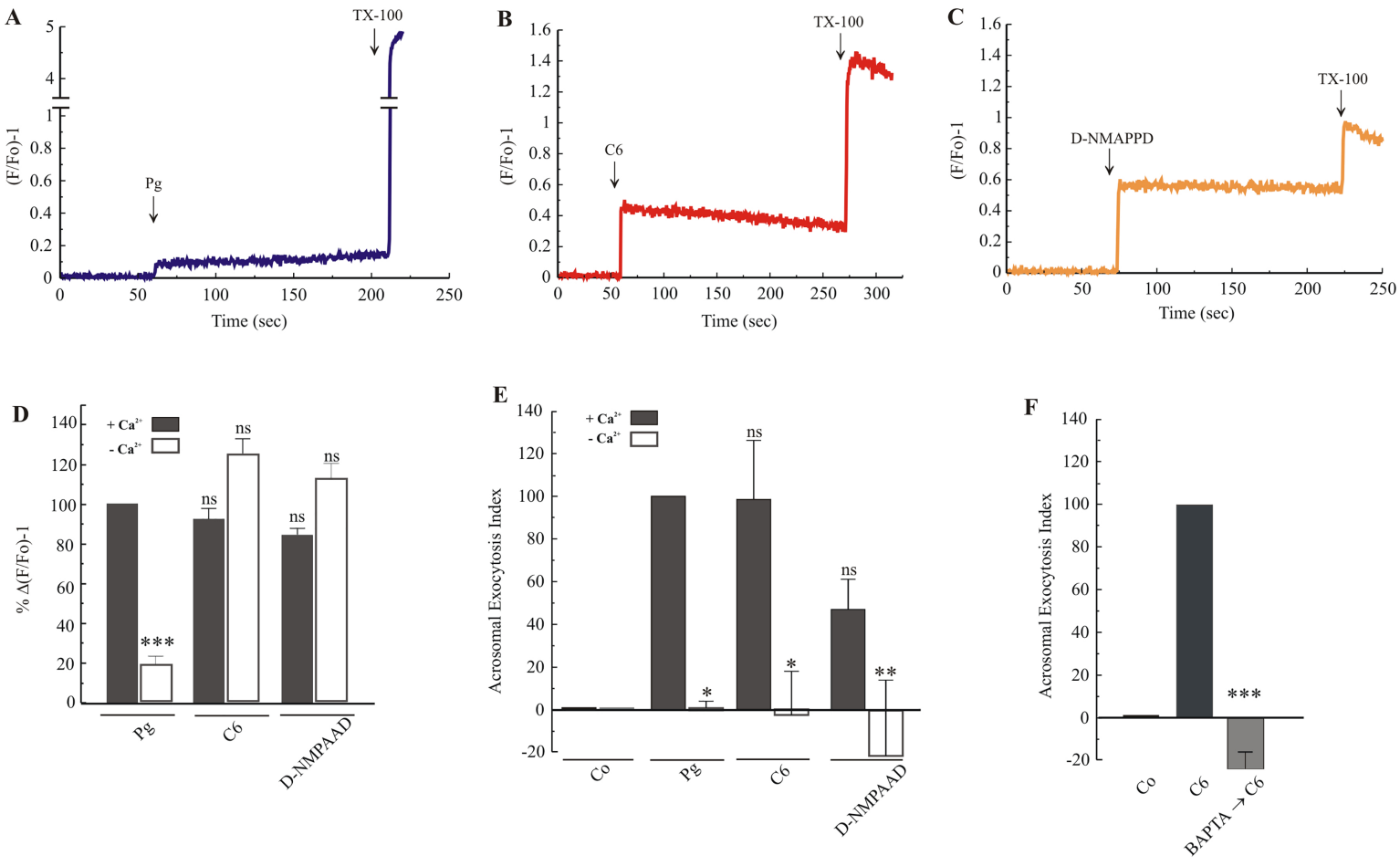
A
TX-100
Pg
(F/Fo)-1
Time (sec)
B
TX-100
C6
(F/Fo)-1
Time (sec)
C
TX-100
D-NMAPPD
(F/Fo)-1
Time (sec)
D
+ Ca2+
- Ca2+
% Δ(F/Fo)-1
ns
***
Pg
C6
D-NMPAAD
E
+ Ca2+
- Ca2+
Acrosomal Exocytosis Index
ns
*
**
Co
Pg
C6
D-NMPAAD
F
Acrosomal Exocytosis Index
***
Co
C6
BAPTA → C6

Figure 6

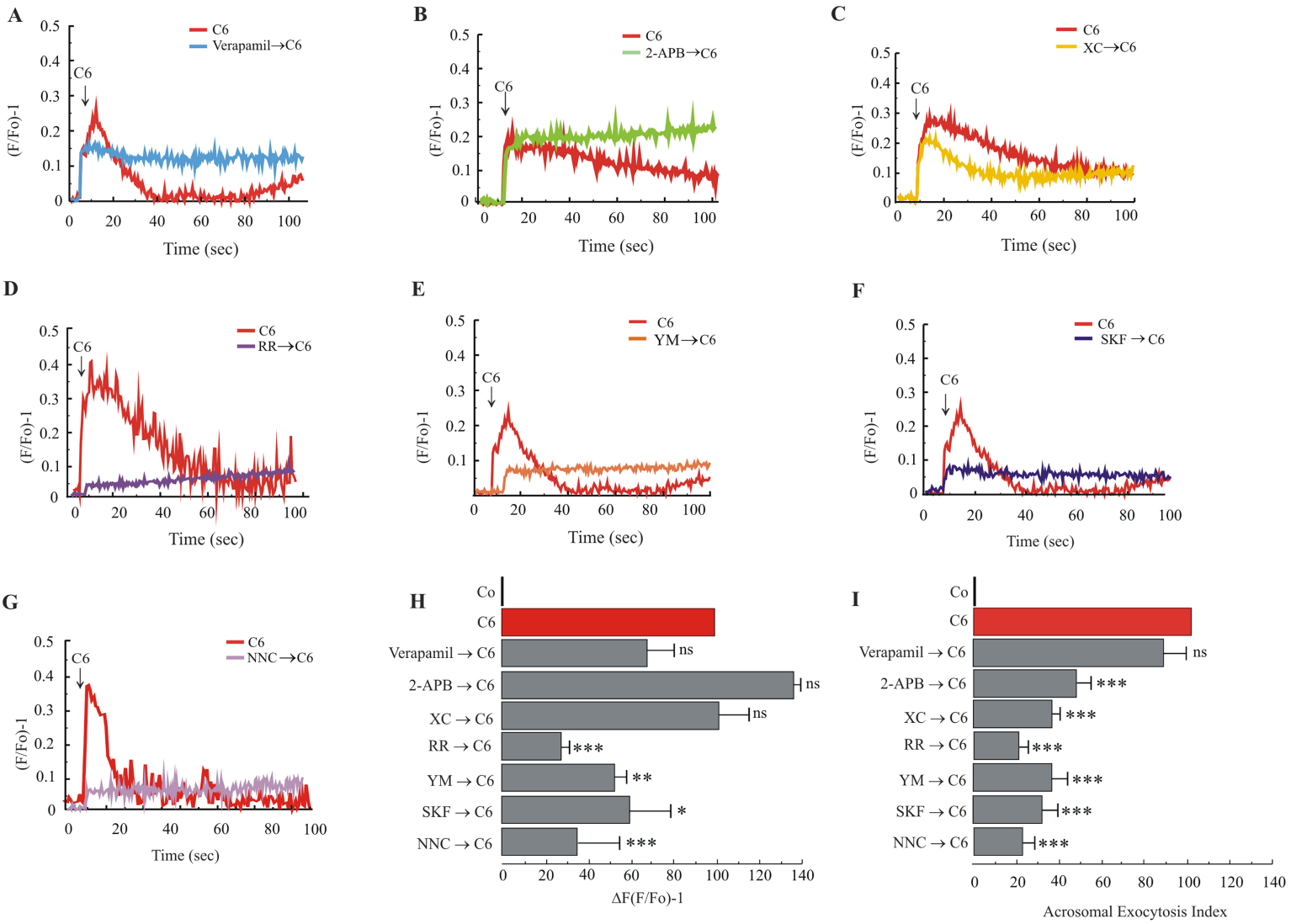
A
C6
Verapamil→C6
C6
(F/Fo)-1
Time (sec)
B
C6
2-APB→C6
C6
(F/Fo)-1
Time (sec)
C
C6
XC→C6
C6
(F/Fo)-1
Time (sec)
D
C6
RR→C6
C6
(F/Fo)-1
Time (sec)
E
C6
YM→C6
C6
(F/Fo)-1
Time (sec)
F
C6
SKF→C6
C6
(F/Fo)-1
Time (sec)
G
C6
NNC→C6
C6
(F/Fo)-1
Time (sec)
H
Co
C6
Verapamil → C6
2-APB → C6
XC → C6
RR → C6
YM → C6
SKF → C6
NNC → C6
ns
ns
ns
***
**
*
***
ΔF(F/Fo)-1
I
Co
C6
Verapamil → C6
2-APB → C6
XC → C6
RR → C6
YM → C6
SKF → C6
NNC → C6
ns
***
***
***
***
***
***
Acrosomal Exocytosis Index

Figure 7

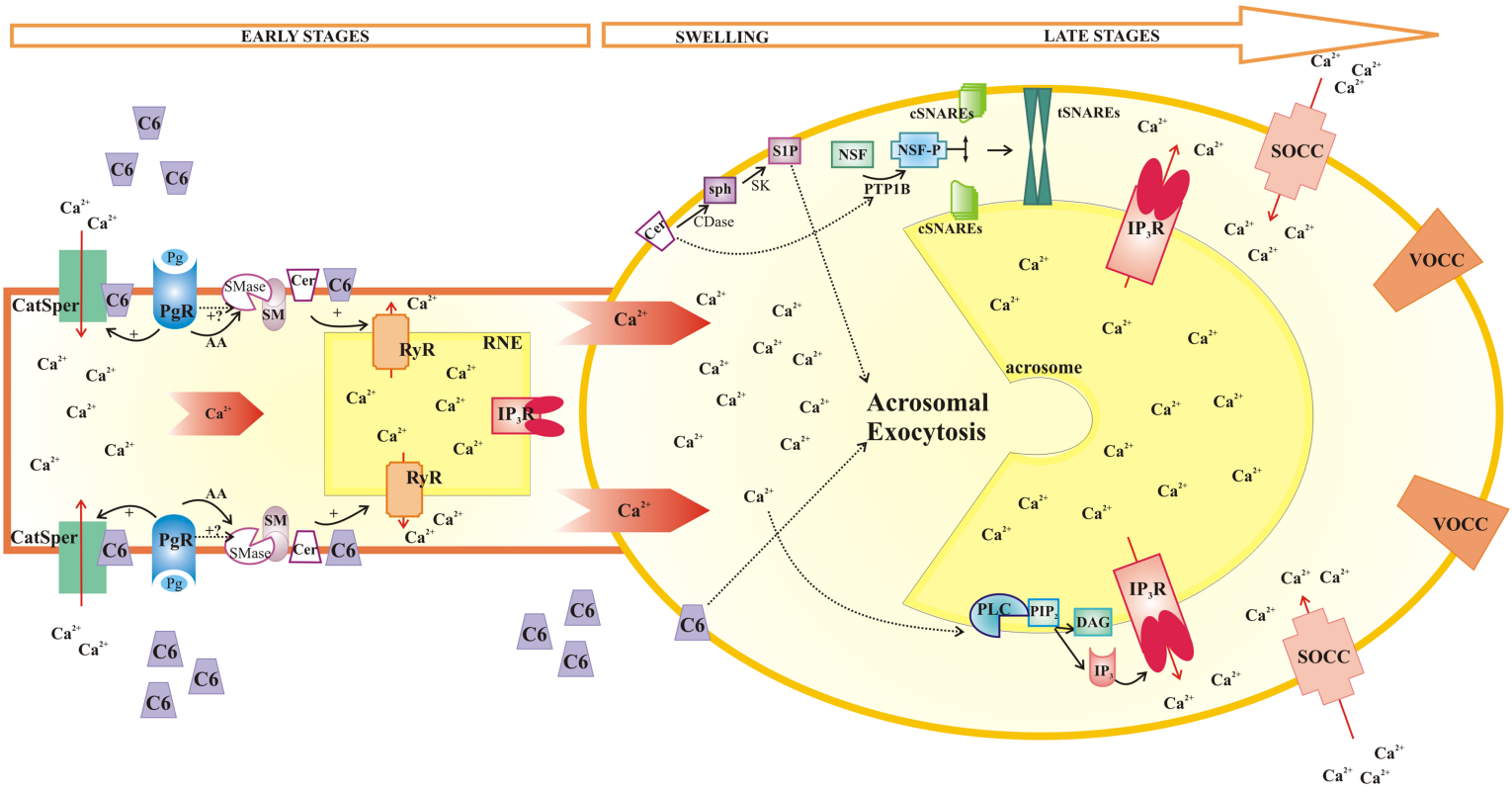
EARLY STAGES
SWELLING
LATE STAGES
C6
Ca2+
CatSper
PgR
Pg
SMase
SM
Cer
AA
+?
RyR
RNE
IP3R
cSNAREs
tSNAREs
S1P
NSF
NSF-P
PTP1B
sph
SK
CDase
Cer
SOCC
VOCC
acrosome
Acrosomal Exocytosis
PLC
PIP2
DAG
IP3

Figure 8